GEOLOGICA CARPATHICA, DECEMBER 2023, 74, 6, 469–488 https://doi.org/10.31577/GeolCarp.2023.25

Surviving from transgression to regression of Lake Pannon: Fan deltas of the Nemčiňany Fm. persisted across the rifting until the post-rift stage of the Danube Basin, western Slovakia

MICHAL ŠUJAN[1,✉], KISHAN AHERWAR[1], ANDREJ CHYBA[2], BARBARA RÓZSOVÁ[1], RÉGIS BRAUCHER[3], MARTIN ŠUJAN[4], FRANTIŠEK ŠIPKA[4] and ASTER TEAM[3]

[1]Department of Geology and Paleontology, Faculty of Natural Sciences, Comenius University in Bratislava, Ilkovičova 6, 842 15 Bratislava, Slovakia; ✉michal.sujan@uniba.sk
[2]Institute of Chemistry, Slovak Academy of Sciences, Dúbravská cesta 9, 845 38 Bratislava, Slovakia; andrej.chyba@savba.sk
[3]CNRS-IRD-Collège de France-INRA, CEREGE, Aix-Marseille Univ., 13545 Aix-en-Provence, France; braucher@cerege.fr
[4]EQUIS Ltd., Račianska 57, 831 02 Bratislava, Slovakia; equis@equis.sk

(Manuscript received October 31, 2023; accepted in revised form January 19, 2024; Associate Editor: Igor Broska)

Abstract: Successions deposited under rifting and post-rift settings of an isolated epicontinental basin often exhibit contrasting characteristics. Facies linked to transgression during basin rifting are typically locally sourced fan deltas transporting coarse-grained sediment, whereas the post-rift setup generally involves a normal regression marked by more extensive catchments, sediment sourced from greater distances, and an overall decrease in average grain size compared to the transgressive facies. In this study, we present a specific scenario based on a sedimentological, stratigraphic, and authigenic $^{10}Be/^{9}Be$ analysis of the Nemčiňany Formation, an Upper Miocene fan deltaic succession in the eastern Danube Basin, Slovakia. Deposition of the Nemčiňany Fm. was initiated shortly after ~11.6 Ma by the fourth rifting phase of the Pannonian Basin System, triggering the transgression of Lake Pannon. The depositional system persisted until ~9.6 Ma, likely balancing the increased accommodation rate with sediment supply in the shallow lake area situated on a basement high. Subsequently, a relative decrease in the accommodation rate prompted the progradation of shelf-slope scale clinoforms, originating from the Nemčiňany depositional system, toward the center of the Komjatice depression at ~9.4 Ma, resulting in a normal regression of Lake Pannon. The persistence of the Nemčiňany fan delta system, unlike common stratigraphic patterns, was associated to the high sediment supply yielded by the paleo-Hron river, which entered the basin in the study area. These observations underscore the need for caution in predicting provenance shifts during changes in geodynamic stages of a basin.

Keywords: facies analysis, authigenic $^{10}Be/^{9}Be$ dating, cosmogenic nuclides, Pannonian Basin System, Late Miocene, supercritical flow bedforms

Introduction

Rifting of basins represents a fundamental process that influences the geometry and composition of the continental crust (Allen & Allen 2013; Cloetingh et al. 2015). The cycle of basin formation and deformation plays a pivotal role in the development of heavily populated lowlands, the genesis of petroleum and geothermal resources, as well as in the emergence of geohazards linked to seismic activity and land subsidence (Cloetingh et al. 2023). Therefore, comprehending the intricacies of rift formation process holds significant importance for prediction of the distribution of resources and assessment of geohazards.

A distinctive depositional architecture for the early stages of rifting involves the creation of locally-sourced alluvial fan to fan delta systems (Burns et al. 1997; Catuneanu 2006; Matenco & Haq 2020). These systems are marked by substantial sediment influx originating from footwalls that become exposed due to fault activity associated with the rifting process (Postma 2009). The deposition of coarse-grained sediment commonly seen in fan deltas, which characterizes transgressive system tracts, is typically replaced in the post-rift stage by regressive deltas with sediment sourced from much farther distances (Balázs et al. 2016; Matenco & Haq 2020). This phenomenon reflects the establishment of catchments at a regional scale due to the waning of fault activity and the filling of basins.

Given that epicontinental rifted basins are frequently isolated and detached from the global ocean, establishing a chronostratigraphic framework for a rifting succession via biostratigraphy is challenging (Kováč et al. 2018). The coarse-grained nature and secondary alterations can impede the effective use of magnetostratigraphy, while volcanic layers suitable for dating are inherently elusive (Langereis et al. 2010; Kelder et al. 2018). When conventional geochronological methods encounter difficulties, new techniques are on hand, such as the authigenic $^{10}Be/^{9}Be$ dating method (Bourlès et al. 1989; Lebatard et al. 2008).

In this study, we focus on fan deltas deposited as a result of the Late Miocene rifting of the Pannonian Basin System (PBS; Fig. 1), which led to formation of the largest late Cenozoic lake of Europe – Lake Pannon (Magyar et al. 1999; Harzhauser & Mandic 2008; Magyar 2021). The aims of the study are to promote understanding of the evolutionary process during this phase of rifting by (1) a reevaluation of the Nemčiňany Fm. coarse-grained deltaic facies in the eastern Danube Basin and (2) resolving their age and stratigraphic position using authigenic $^{10}Be/^{9}Be$ geochronology. We employ facies analysis on two key outcrops, Tajná and Nemčiňany sites. While the sites were previously examined (Baráth & Kováč 1995; Kováč et al. 2008), recent advancements in the analysis of fan delta depositional processes have imposed fresh demands on the existing interpretations. Moreover, the Late Miocene period was traditionally considered as a post-rift stage in evolution of the PBS (e.g., Lankreijer et al. 1995), but a growing pile of evidence including this study indicates the existence of a rifting phase in the region after ~11.6 Ma (Balázs et al. 2017; Šujan et al. 2021b). The fan delta facies association

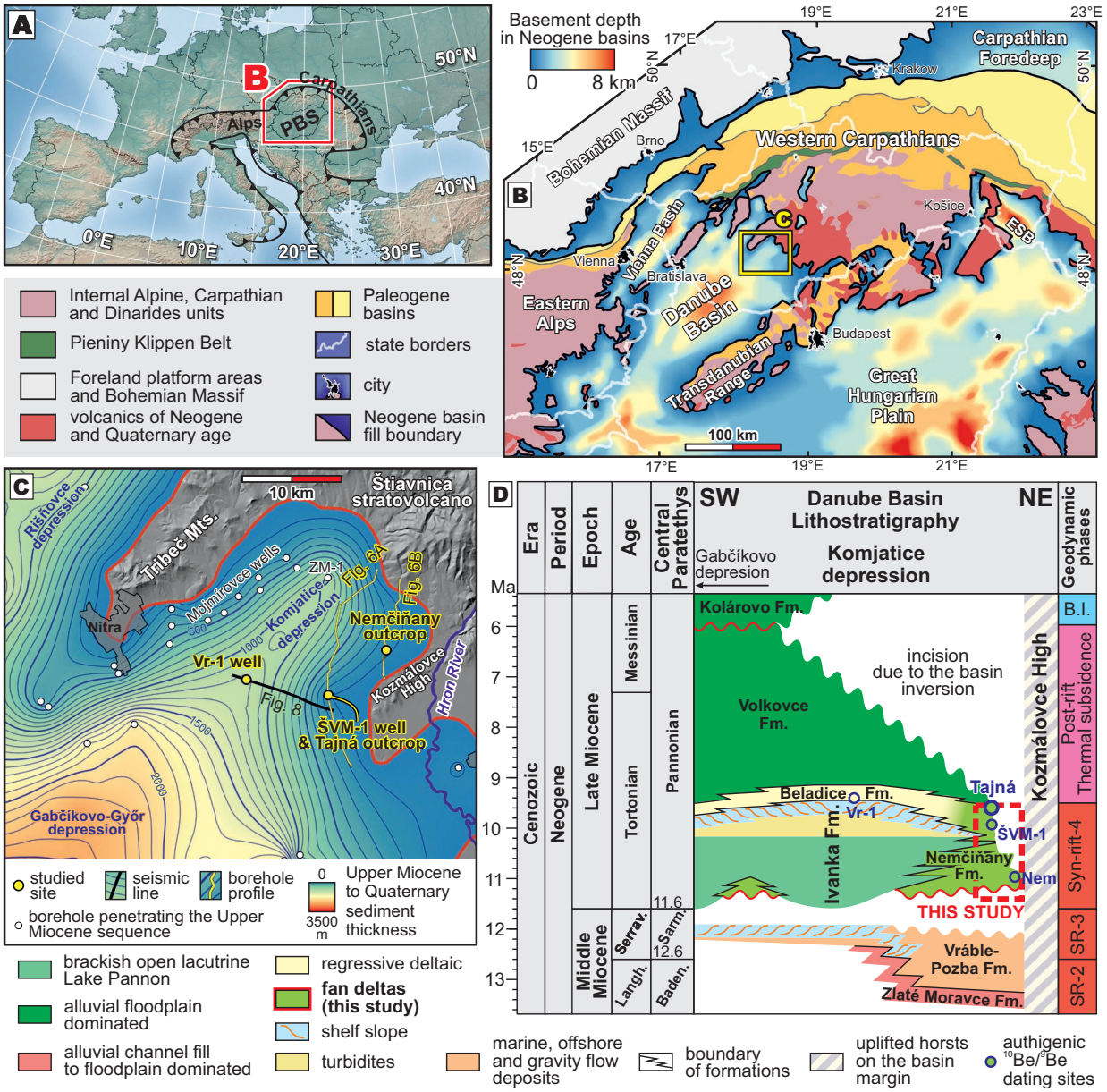

Fig. 1. Location of the study area and its lithostratigraphy: **A** — Pannonian Basin System within Central Europe. **B** — Neogene basins in the northern Pannonian domain and location of the Danube Basin, modified from Šujan et al. (2021b). Abbreviations: ESB – East Slovakian Basin. **C** — Komjatice depression in the northeastern Danube Basin and studied sites. Miocene to Quaternary sediment thickness map Sztanó et al. (2016). **D** — Lithostratigraphy of the Komjatice depression, modified from Šarinová et al. (2018). Circles indicate the stratigraphic position of the dated sites. Geodynamic phases according to Šujan et al. (2021b). Abbreviations: Langh. – Langhian, Serrav. – Serravallian, Baden. – Badenian, Sarm. – Sarmatian, B.I. – basin inversion.

determined on outcrops was correlated in the basin fill using a set of borehole profiles. The chronostratigraphy of the studied fan delta succession is established by new authigenic $^{10}Be/^{9}Be$ dating results supported by a review of the previously published ages (Šujan et al. 2016).

Geological setting

The Pannonian Basin System is a back-arc superbasin formed during the Miocene in the region between the Eastern Alps, Carpathian Mts. Arc, and the Dinarides (Horváth 1993; Horváth et al. 2015; Kováč et al. 2017; Tari et al. 2023; Fig. 1A, B). Rifting of the basin resulted in general from subduction pull of the North European plate below the Carpathian orogenic wedge and extrusion of the ALCAPA microplate towards the northeast. Diapiric upwelling of asthenospheric mantle led to crustal thinning and weakening. This process was stepwise, varied temporally and spatially, and hence the depositional record of specific sub-basins differs in number of events and character of preserved rifting phases (Balázs et al. 2016; Kováč et al. 2017; Šujan et al. 2021b).

The relative wealth of stratigraphic and geochronological data made it possible to distinguish four separate rifting phases in the Danube Basin, the northeasternmost subbasin of the PBS (Šujan et al. 2021b; Fig. 1B). As a transition towards the basin-and-range structure formed within the Western Carpathians, fingerlike depressions with prevailing NW–SE orientation were created in the Danube Basin during the rifting (Nemčok & Lexa 1990; Kováč & Hók 1993). This study focuses on the Komjatice depression, a northeastern fingerlike embayment situated between the Tribeč Mts. (Fig. 1C), composed of pre-Cenozoic rocks, and the Kozmálovce High consisting of Middle Miocene volcanites and volcaniclastics. The depression experienced significant subsidence during the 2nd and 3rd rifting phases (~13.8–12.6 Ma; ~12.6–11.6 Ma), associated with marine, coastal and terrestrial environments of the Zlaté Moravce and Vráble–Pozba fms. (Šarinová et al. 2018; Fig. 1D).

The transition of the Middle and Late Miocene is marked by a base level fall and isolation of the PBS from neighboring marine basins, which gave birth to Lake Pannon (Magyar et al. 1999; Harzhauser & Mandic 2008). Apart from possible glacioeustatic forcing (Harzhauser et al. 2004; Lirer et al. 2009), uplift of the Eastern Carpathians clearly played an important role in this process (Vasiliev et al. 2010; ter Borgh et al. 2013). A compressional event marked the transition by an angular unconformity, visible in seismic lines across the PBS and also in the Danube Basin (Horvath & Cloetingh 1996; Balázs et al. 2016; Šujan et al. 2021b). The following Late Miocene rifting, constrained to ~11.6–9.5 Ma, is traceable as offset of up to 500 m on some major faults in the basin fill (Šujan et al. 2021b). The resulting differentiation of the Lake Pannon bottom formed a complex framework of deep basin depocenters across the PBS, divided by submerged highs and horsts exposed subaerially as islands (Balázs et al. 2018). The rifting of the Danube Basin was replaced by a post-rift stage after ~9.5 Ma (Šujan et al. 2021b), marked by a general vanishing of fault-controlled subsidence and prevailing thermal subsidence as a result of relaxation, cooling and contraction of the lithosphere (Allen & Allen 2013; Cloetingh et al. 2015; Fig. 1D).

The Pannonian rifting induced the accumulation of the Nemčiňany Fm., which represents an alluvial fan to fan delta succession deposited during the transgression of Lake Pannon (Sztanó et al. 2016), and is the subject of this study. The corresponding strata were previously classified to the Pliocene age (Priechodská & Harčár 1988; Vass et al. 1990; Baráth & Kováč 1995; Kováč et al. 2006, 2008), based on:

- the usage of the stages Pontian, Dacian and Romanian in the Central Paratethys stratigraphy – a recently abandoned practice (Sztanó et al. 2016; Magyar 2021; Šujan et al. 2021b), since the stages were defined using paleobiological and stratigraphic events in the Eastern Paratethys (Stoica et al. 2013; Van Baak et al. 2015), which was at that time isolated from the Central Paratethys;
- the incorrect assignment of the corresponding deposits to the younger Volkovce Fm. (Priechodská & Harčár 1988; Baráth & Kováč 1995), which constitutes the uppermost part of the Upper Miocene sequence, reinterpreted as alluvial in the current lithostratigraphy (Sztanó et al. 2016); the alluvial terrestrial origin of the Volkovce Fm. and lateral transition of the Nemčiňany Fm. with brackish open lacustrine facies excludes affinity of these two formations;
- the assumption of deposition of the fan delta deposits as a regressive system tract of Lake Pannon (Kováč et al. 2006), despite this process of regression was temporarily not well constrained at that time due to the absence of a sequence-stratigraphic model supported by geochronological data.

The transgression of Lake Pannon led to the spatially extensive deposition of open lacustrine shallow to deep water Ivanka Fm., which was later replaced by the regressive deltaic Beladice Fm. The process of normal regression was diachronous due to the shelf-slope progradation across the Danube Basin between ~10.0–8.7 Ma (Magyar et al. 2013; Sztanó et al. 2016; Fig. 1D).

Both studied outcrops are situated at the southeastern margin of the Komjatice depression, where denudation related to the Pliocene basin inversion caused the exposure of this lowermost Upper Miocene stratigraphic member at the surface. The Tajná outcrop was the place of drilling for the ŠVM-1 Tajná fully cored well, elaborated by Kováč et al. (2006, 2008). The correlation of the Tajná site towards the basin fill is performed using a seismic line between the ŠVM-1 Tajná and Vráble-1 (Vr-1) wells. The authigenic $^{10}Be/^{9}Be$ dating was applied by Šujan et al. (2016) to the samples from the Nemčiňany outcrop and the ŠVM-1 Tajná well (both Nemčiňany Fm.) and to the cores from the Vráble-1 well (Beladice Fm.; Fig. 1C, D), which are included in the discussion of this paper.

Methods

Sedimentology and stratigraphy

This study provides sedimentological analysis of two sites. The Tajná site is an abandoned quarry ca. 10 m in height and 75 m in width exposing a single wall (48.2576°N, 18.3811°E; Suppl. Fig. S1). A detailed logging was performed together with a scheme of facies distribution at the Tajná site. The Nemčiňany quarry (48.3046°N, 18.4551°E) consists of three levels (Suppl. Fig. S1), the second of which serves for occasional present-day excavation of gravel. The up to 15 m high and ca. 200 m wide fresh outcrop was a subject of drawing of facies distribution schemes. Only a generalized log of the Nemčiňany site was created due to the problematic accessibility of the vertical wall and is included in the Supplementary material. The high spatial variability and considerable size of the observed facies favor sedimentological scheme as a better tool for depiction of the stratal patterns and facies distribution. The facies analysis was performed according to Stow (2005) considering up-to-date sedimentological knowledge for upper-flow regime bedforms provided by Cartigny et al. (2014), Postma & Cartigny (2014) and Slootman et al. (2021). Orientation of 61 foreset beds was measured using a geological compass at the Nemčiňany site.

The fan delta facies association, established on outcrops, was correlated using lithological profiles of 27 boreholes, summarized in Suppl. Table S1. The two north-south oriented geological sections were constructed using the borehole profiles, in order to represent the occurrence of the Nemčiňany Fm. These data were obtained from manuscripts located in the Geofond archive of the State Geological Survey of Dionýz Štúr and are listed in Suppl. Table S1. The lithology was unified using a code of 9 lithological classes, including a distinction between subaerial and subaquatic muddy lithotypes (e.g., Aslan & Autin 1999; Campo et al. 2016). Units up to a thickness of 0.5 m could be occasionally distinguished in the lithological log descriptions. However, the wells were mostly drilled for hydrogeological exploration, therefore the lithological descriptions are frequently very general and with a depth resolution to 2–5 m thick units. The coarse-grained Nemčiňany Fm. and muddy Ivanka Fm. are repeatedly alternating laterally and vertically, what is the reason for their depiction as a single horizon in the geological sections. The area is characteristic by a cyclic alteration of the Nemčiňany and Ivanka fms. in a vertical section, both are therefore shown as a single horizon.

Authigenic $^{10}Be/^{9}Be$ dating

The application of the authigenic $^{10}Be/^{9}Be$ dating method enables the determination of the depositional age of a sedimentary layer up to 14 Ma, given that specific conditions are met (Bourlès et al. 1989; Lebatard et al. 2008; Šujan et al. 2016). The method is based on the radioactive decay of atmospheric cosmogenic radionuclide ^{10}Be with a half-life of 1.387±0.01 Ma (Chmeleff et al. 2010; Korschinek et al. 2010). ^{10}Be is produced in the atmosphere by interaction of cosmic rays with ^{14}N and ^{16}O and rapidly transferred to the hydrosphere, where it mixes with the isotope ^{9}Be (Raisbeck et al. 1981; Measures & Edmond 1983; Brown et al. 1992). ^{9}Be originates from weathering of rocks and is used for normalization of ^{10}Be concentration (Wittmann et al. 2012). Both isotopes are incorporated under oxic conditions in oxyhydroxides forming the authigenic rims around sedimentary particles, which are transported in a water column (Willenbring & von Blanckenburg 2010; Singleton et al. 2017; Wittmann et al. 2017). The authigenic $^{10}Be/^{9}Be$ ratio changes proportionally with depositional age after sedimentation if the system remains chemically closed.

The distinct origins of the two beryllium isotopes pose challenges in employing the method, as the initial ratio is specific to each site, influenced by the varying chemical compositions and ^{9}Be content in weathered rocks on the Earth's surface (Willenbring & von Blanckenburg 2010). The delivery of ^{9}Be into an offshore sedimentary environment is driven by the proximity of a terrestrial source (Wittmann et al. 2017; Kong et al. 2021), while the sedimentation rate and pace of burial play a significant role in penecontemporaneous ^{10}Be enrichment (Aherwar et al. 2021). The redeposition of older mud with preserved authigenic rims can lead to apparent older ages in both alluvial and deep basin settings (Šujan et al. 2023a, b). Two initial authigenic $^{10}Be/^{9}Be$ ratios were established for the Danube Basin, one for lacustrine offshore environments and the latter for delta top to alluvial facies (Šujan et al. 2016). The research conducted in the basin suggests that despite the recognized potential complications associated with application of the method, the initial ratios for the mentioned environments remained stable during the time period of ~11.6–6.0 Ma (Šujan et al. 2016, 2020; Joniak et al. 2020), unless affected by redeposition.

This study provides radiometric ages of five new samples taken from the Tajná site. The samples originate from muddy overbank deposits. Dried and crushed mud of the weight of ~2.25 g per sample underwent leaching of the authigenic phase using a solution of acetic acid, hydroxylamonium hydrochloride (NH_2OH–HCl) and demineralized water. An aliquot was taken from the resulting solution for ICP-MS measurements of total beryllium concentration. The LGC commercial ICP-MS beryllium standard with the isotopic ratio ~$3–4\times10^{-15}$ was added to the main fraction of the solution as a carrier. Column chromatography according to Merchel & Herpers (1999) was applied to separate beryllium from other elements. The purified samples were oxidized in an oven, mixed with niobium powder and filled to copper cathodes for accelerator mass spectrometer (AMS) measurements on the French national AMS facility ASTER at CEREGE (Aix-en-Provence, France) (Arnold et al. 2010). For a detailed description of the sample processing, the reader is asked to see the Supplementary material.

Results

Sedimentology

Properties and interpreted depositional processes of all documented lithofacies are summarized in Table 1. The orientation of analyzed outcrop walls is depicted in Suppl. Fig. S1.

Tajná outcrop – fan delta topset facies

Description:

All gravel clasts present at the site are rounded to well rounded (Table 1). The lower and middle part of the outcrop consists mainly of lenticular units of the lithofacies Gt with a concave erosional base, made up of clast-supported gravel arranged into a few centimeters thick trough cross-stratified beds (Figs. 2, 3). Intraclasts of mud with up to few decimeters in diameter are present commonly. The beds onlap on the basal surface and may form a partly convex shape in a section oriented more oblique to the axis of a channel-shaped base (Fig. 2). The sections perpendicular to a channel-shaped unit axis are ~10–15 m wide, thickness of an individual unit reaches ~0.5–2.0 m and amalgamation is a common feature (Figs. 2, 3A).

The Gt units are locally separated by intercalations of few decimeters thick tabular bodies consisting of massive clast- to matrix-supported rounded gravel with a common normal gradation (Gmm), or by massive clast-supported gravel forming ~0.5–1.0 m thick tabular or lenticular units (Gmk; Fig. 3F). The lithofacies Gt is frequently incised into Gmm and Gmk and erodes them (Fig. 2).

The amalgamated Gt units are separated in the middle part of the outcrop by a horizon consisting of medium-grained planar cross-stratified sand (Sp) and ripple-cross stratified fine-grained sand (Sr; Fig. 3E).

The northern (left) part of the outcrop wall exposes a muddy horizon, which is discontinuous, likely due to erosion (Fig. 2). It consists of alteration of light brown to reddish subhorizontally laminated mud (Fl) and of light grey massive mud (Fm), sometimes with the presence of a few millimeters thick sandy laminae (FSm; Fig. 3C, D). Seven centimeters thick ripple cross-stratified fine-grained sandy layer also appears.

The upper portion of the outcrop is sandier and gravel content decreases (Figs. 2, 3A). Planar cross-stratified sands (Sp), locally with granules, and planar cross-stratified gravels (Gp) are more common. Cross-stratified units ~1–2 m thick appear (Stb), composed of foresets with various grain size, sandy and less gravelly, and with internal angular contacts. Gt units are less frequent in the upper part of the outcrop and reach a thickness of ~0.3–0.5 m. Tabular beds of massive matrix-supported gravel (Gmm) are seldom.

Interpretation:

The Gt units could be considered as channels gradually filled by bedload-dominated traction currents, accumulating downstream-accreted bars (Boothroyd & Ashley 1975; Gobo et al. 2015; Martini et al. 2017). The channels were subject to

Table 1: List of lithofacies documented on the Tajná and Nemčiňany outcrops, their properties and interpreted depositional processes.

Code	Lithology, structure, texture and geometry	Depositional processes
Gmm	massive clast- to matrix-supported rounded gravel, commonly normally graded, sandy matrix, granules to pebbles, less boulders, forming decimeters thick horizontal tabular bodies	hyperconcentrated flow (Pierson & Costa 1987; Brenna et al. 2020)
Gkm	massive clast-supported rounded gravel, moderately to well sorted, granules and pebbles, forming ~0.5–1.0 m thick amalgamated tabular and lenticular bodies, frequently amalgamated, infrequent muddy-sandy intraclasts	debris flood (Church & Jakob 2020; Brenna et al. 2020)
Gt	clast-supported gravel arranged into trough-cross stratified beds a few centimeters thick, rounded granules to pebbles, moderately to well sorted in a single bed, arranged into lenticular bodies up to a few meters thick with concave erosional base, frequent large intraclasts at the base and within the body	channelized traction current, accretion of a channel-fill bar (Boothroyd & Ashley 1975; Gobo et al. 2015; Martini et al. 2017)
Gp	clast-supported gravel arranged into planar cross-stratified beds, rounded granules to pebbles, subangular to rounded, forming decimeters thick horizontal tabular bodies	traction current forming gravelly dunes (Allen 1982; Leclair & Bridge 2001)
Gcp	clast- to matrix-supported gravel arranged into lenticular units few meters thick and up to 10 m wide, with concave bedding at the base changing upwards to a convex shape, bounded by erosional surfaces, rounded pebbles	upper flow regime bedform – chute-and-pool (Cartigny et al. 2014; Slootman et al. 2021)
Gcs	clast- to matrix-supported gravel forming backsets climbing upwards a foreset slope, massive to tabular, units a few meters thick, with sharp erosional undulated base, frequent soft-sediment deformations at the base	upper flow regime bedform – cyclic steps (Cartigny et al. 2014)
Stb	sand and less gravel arranged in planar inclined beds, with various grain sizes, forming 1–2 m thick and ca. 10 m wide lenticular bodies, with reactivation surfaces marked by angular contacts	unit-bar in a channel (Reesink et al. 2018)
Sp	planar cross-stratified medium- to fine-grained sand in a few decimeters thick tabular bodies	traction current forming 2D dunes (Allen 1982; Leclair & Bridge 2001)
Sr	unidirectional ripple-cross stratified fine sand to muddy sand	slow traction current (Allen 1982; Robert & Uhlman 2001; Yawar & Schieber 2017)
FSm, Fm	light grey massive mud with sandy laminae, or massive light grey mud	deposition from suspension of a high mud- concentrated waning flow in an oxbow lake, on proximal floodplain or on a marsch (Toonen et al. 2011; Baas et al. 2016)
Fl	subhorizontally laminated light brown to reddish mud	deposition from a slow traction current or from suspension in a proximal floodplain or on a marsch (Aslan & Autin 1999; Yawar & Schieber 2017)

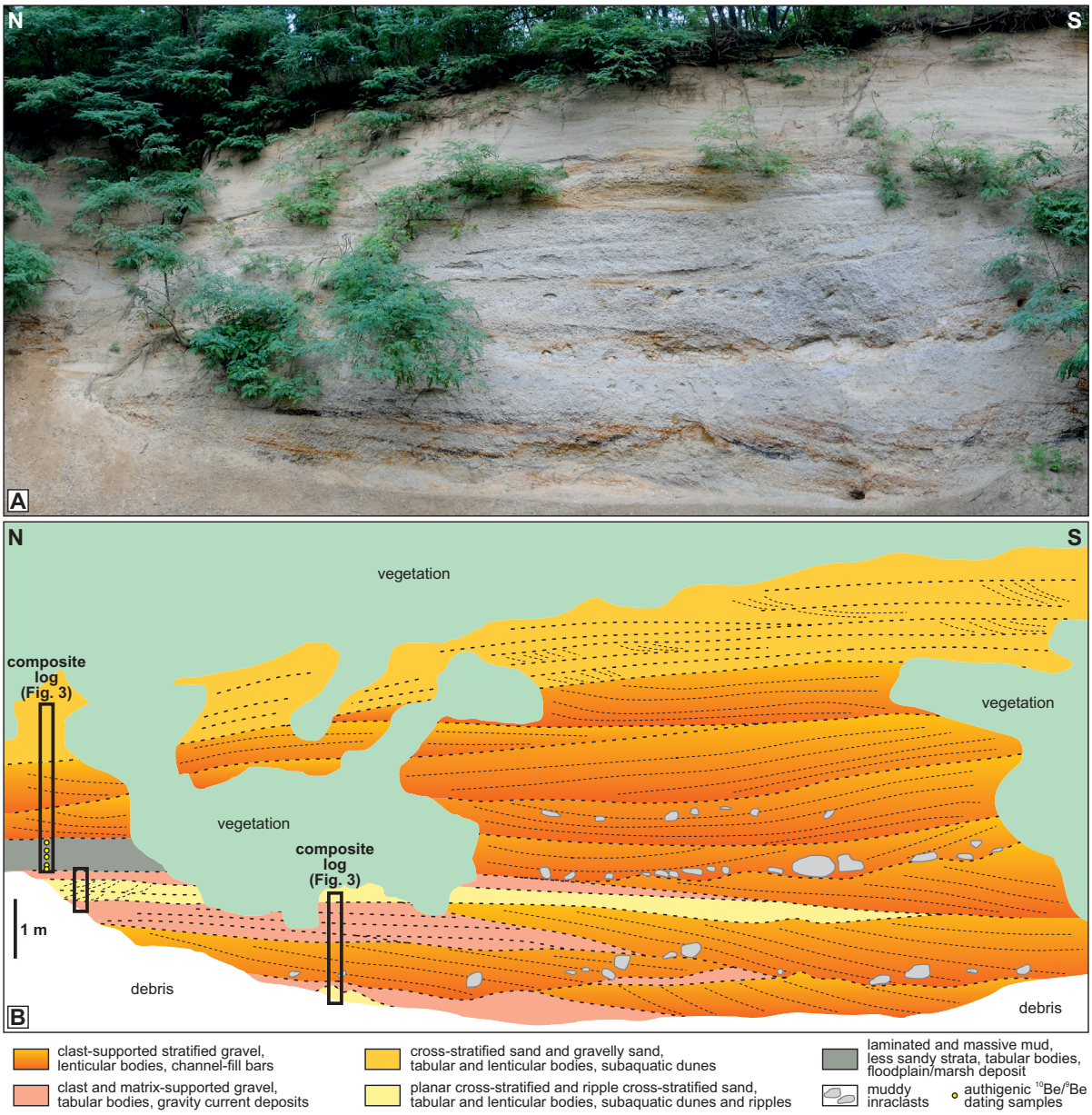

Fig. 2. A scheme of facies distribution in the Tajná site outcrop wall, showing a fan delta topset facies association. The geometry of boundaries in the upper portion is slightly deformed by the wide-angle panoramic photograph. Suppl. Fig. S1 shows the morphology of the quarry and location of the depicted outcrop wall. Site location in Fig. 1C.

debris floods with high bedload transport, causing that almost all grain sizes were transported and deposited as bedload-carpet accretion of the lithofacies Gmk (Manville & White 2003; Brenna et al. 2020; Church & Jakob 2020). The traction currents confined in channels were alternated by event-like unconfined subaerial hyperconcentrated flows (Gmm; Pierson & Costa 1987; Brenna et al. 2020).

The muddy horizon in the interval 4.8–5.9 m (Fig. 3A) exhibits features of alteration of deposition from very slow traction currents to suspension settling from a standing water column (Fl; Aslan & Autin 1999; Yawar & Schieber 2017), and of rapid sedimentation from suspension by high muddy sediment-concentrated flow (Fm, FSm; Toonen et al. 2012; Baas et al. 2016).

The planar cross-stratified sand and gravel (Sp, Gp) is a result of migration of subaquatic 2D dunes (Allen 1982; Leclair & Bridge 2001) and ripple cross-stratified sand (Sr) represents unidirectional flow ripples (Allen 1982; Robert & Uhlman 2001; Yawar & Schieber 2017). The mostly sandy body of Stb exhibit irregular changes in lithology from foreset to foreset, different from a typical dune cross-stratification, and internal angular contacts appear, what indicates deposition of Stb as a unit-bar in a channel (Reesink 2018).

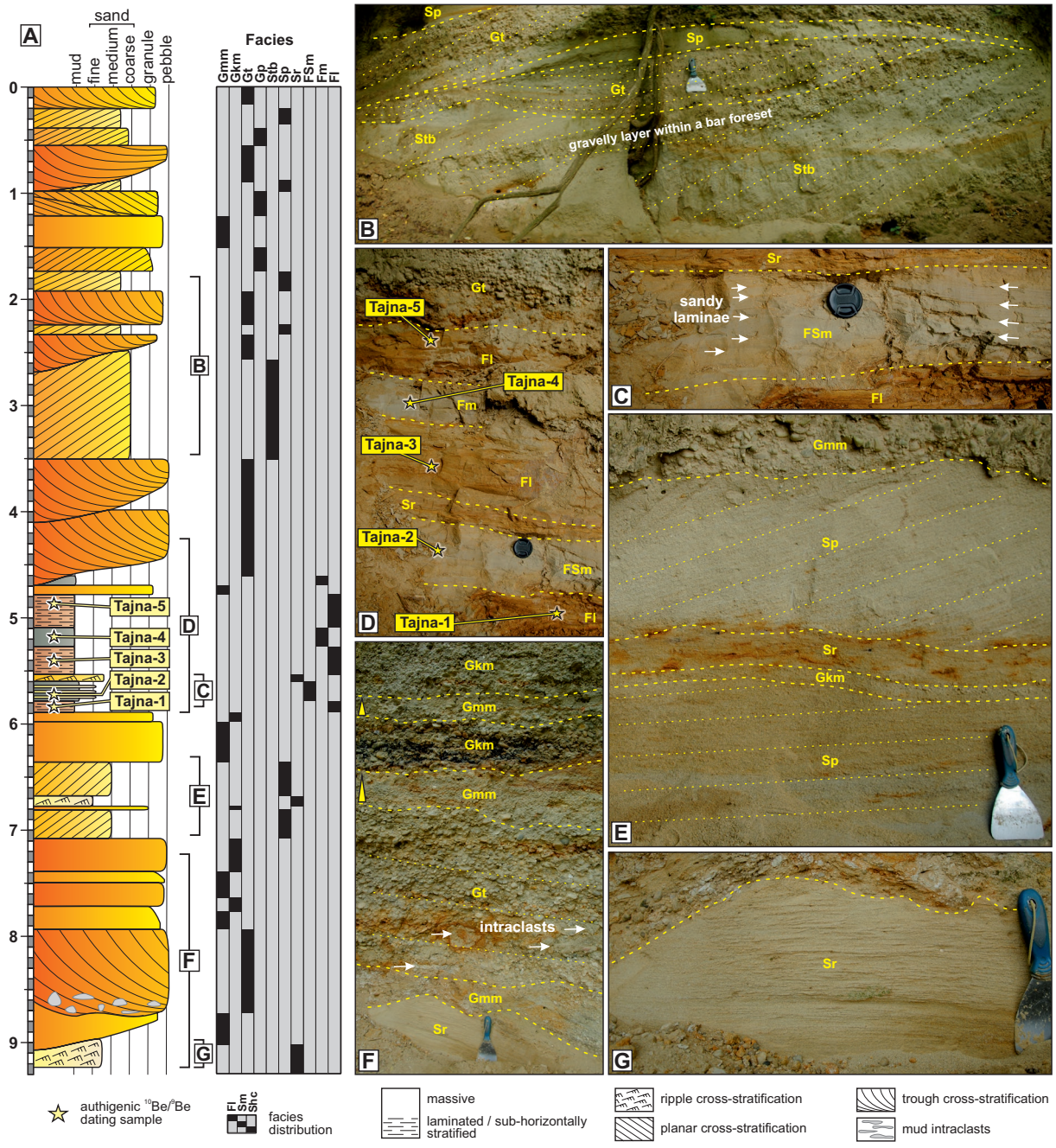

Fig. 3. Sedimentological log of the Tajná outcrop: **A** — vertical distribution of the lithofacies and sampling points for dating. **B–G** — Details of the lithofacies appearance. See Table 1 for the lithofacies codes. Location of the log in Fig. 2.

The described association of processes of the lower and middle part of the outcrop implies its deposition by a braided network of channels with dominant in-channel sedimentation and a high sediment supply to accommodation ratio (Bridge & Lunt 2006). The appearance of event-like high sediment-concentrated flows (Gmm, Gmk) is associated with seasonal floods (Brenna et al. 2020). The overbank deposition of flood-plain facies (Fl, Fm, FSm, Sr) was limited, causing low strength of the riverbanks and a braiding pattern. The upper portion of the outcrop mirrors a decrease of the sediment supply to accommodation ratio, expressed as a lower content of gravel and facies indicating lower transport capacity, with a more common deposition of dunes.

The observed vertical change in facies association could be a result of autogenic migration of the deepest channel axis, and deposition in shallower, more peripheral channels in the case of the upper portion of the outcrop (Postma 2014; Lojka et al. 2016). Since the gravelly-sandy succession alternates with open lacustrine muds at the site (Kováč et al. 2008), it represents a braidplain topset of a fan delta (Postma 2009).

This is expressed in the relatively low dimensions of the channels, with depths of ~0.5–2.0 m. Considering a typical cyclic alteration of the delta progradation and flooding, the observed vertical change of the facies associations at the Tajná site is likely associated with a delta lobe avulsion (Van Dijk et al. 2009).

Nemčiňany outcrop – fan delta forest facies

Description:

The outcrop walls are dominated by two types of units (Suppl. Fig. S2). The first type is indicated as Gcp and comprises lenticular units few meters thick and ~10 m wide (Fig. 4A, B, Table 1). The internal structure shows concave clast- to matrix-supported gravelly beds changing upwards into convex-shaped beds. The individual beds are few centimeters to 15 cm thick. The contacts of individual Gcp bodies are erosive and the units are amalgamated.

The second type of units are gravelly to gravelly-sandy tabular beds of Gcs forming extensive foresets with a dip of 7–20° (Fig. 4A, B, Table 1). The continuous horizons are traceable across the ~35 m high quarry without a topset or bottomset transition. The beds form subsets few meters thick with erosional contacts. The tabular beds are generally inclined towards the west (Suppl. Fig. S2). A closer look into these subsets reveal the presence of backsets with an opposite dip in comparison to the main foresets (Fig. 4D), usually with an erosional base and the lowermost portion composed of massive gravel underlined by liquefaction deformations (Ta; Fig. 5A). The overlying tabular subsets show smooth normal and reverse grain size grading without erosional contacts ($Tb_{4–3a}$; Fig. 5C), changing upwards into a bedding with upward coarsening trends bounded by erosional contacts (Tb_{3b}; Fig. 5B, C) and caped by increasingly pronounced bedding with spacing of few centimeters (Tb_2; Fig. 5D). The Gcs and Gcp units appear separately as multiple one-type facies groups (Fig. 4A, B) or are alternating each other randomly (Suppl. Fig. S3).

Interpretation:

The concave to convex geometry of the lithofacies Gcp implies a deposition of gravel and sand from suspension as an upper flow regime bedform (Cartigny et al. 2014). The lenticular shape and internal bedding pattern corresponds to the definition of chute-and-pools according to Slootman et al. (2021) (Fig. 4C). The backset geometry of the facies Gcs is also a typical feature for deposition in the upper flow regime (Slootman & Cartigny 2020). The several meters thick and ~10 m wide backsets could be associated with the division of facies in a vertical succession, typical for cyclic steps as defined by Postma & Cartigny (2014) (Fig. 4E):

- Ta as massive gravel deposited by a hydraulic jump (transition from supercritical to subcritical flow) over an erosional base and above liquified sediment;
- crudely bedded backsets of $Tb_{4–3a}$ accumulated in a regime of subcritical flow, mirroring variations in the flow velocity without erosion;
- Tb_{3b} representing a subcritical flow with intervals of increasing velocity up to a change from accumulation to erosion;
- Tb_2 showing stratification with a decreasing spacing between bedding planes upwards, as the flow becomes supercritical and erosive with increasing velocity.

Hence, the observed deposits of the Nemčiňany site were accumulated in the upper flow regime, most likely from high-density turbidite flows with supercritical basal layer (Postma & Cartigny 2014). The preservation of convex lamination in chute-and-pool lenses is also characteristic for subaquatic density flows (Slootman et al. 2021). It is worth nothing that the cyclic steps and chute-and-pools dominate the exposed succession and lithofacies representing other depositional processes are minor. The facies association could be classified as a foreset of a high-density turbidity flow-dominated fan delta (Postma 2009).

The good sorting and rounding of the clasts, low variability of upper-flow regime depositional processes, the scale of supercritical-flow bedforms and the foreset height exceeding 35 m indicate a steady depositional system of a relatively large fan delta (Nemec & Steel 1988; Longhitano 2008; Postma 2009). The water column entered by the fan delta had to reach a depth of at least 35 m, and the bedforms with a corresponding order of wavelength were observed on the slopes reaching a height of 80–200 meters (Casalbore et al. 2011; Fricke et al. 2015; Normandeau et al. 2016; Hage et al. 2018; Vendettuoli et al. 2019; Postma et al. 2021). The height is in the mentioned works established mostly based on the vertical distance between topsets and foresets, either observed in depositional record or in recent deltaic examples.

Stratigraphy based on borehole profiles

The analysis of facies at the Tajná and Nemčiňany sites has enabled the attribution of fan deltaic origin to the gravelly–sandy units, alternating with subaquatic lacustrine muds at the eastern flank of the Komjatice depression. The geological sections in Fig. 6 illustrate the frequent alternation of the Nemčiňany Fm. with the open lacustrine Ivanka Formation, characterized by a chaotic distribution pattern. The units demonstrate coarsening upwards trend of a fan delta lobe progradation in a rare case when the precision of the lithological descriptions allowed to distinguish a vertical grain size change. The fan delta units are commonly overlain by variegated muds of subaerial origin, which represent overbank deposition on a braidplain. The thickness of a single fan delta unit mostly ranges from 20 to 35 m, occasionally reaching up to 60 m. However, the amalgamation of several units may not always be identifiable. The intervals of open lacustrine deposition between the fan delta units typically reach 10–40 m, with occurrences exceeding 50 m being rare.

The base of the merged Nemčiňany and Ivanka fms. was mostly not reached by the boreholes. Despite its course is not revealed in detail, the outline of a syncline was discernible to the north of the Tajná site and the Kozmálovce High (Fig. 6C)

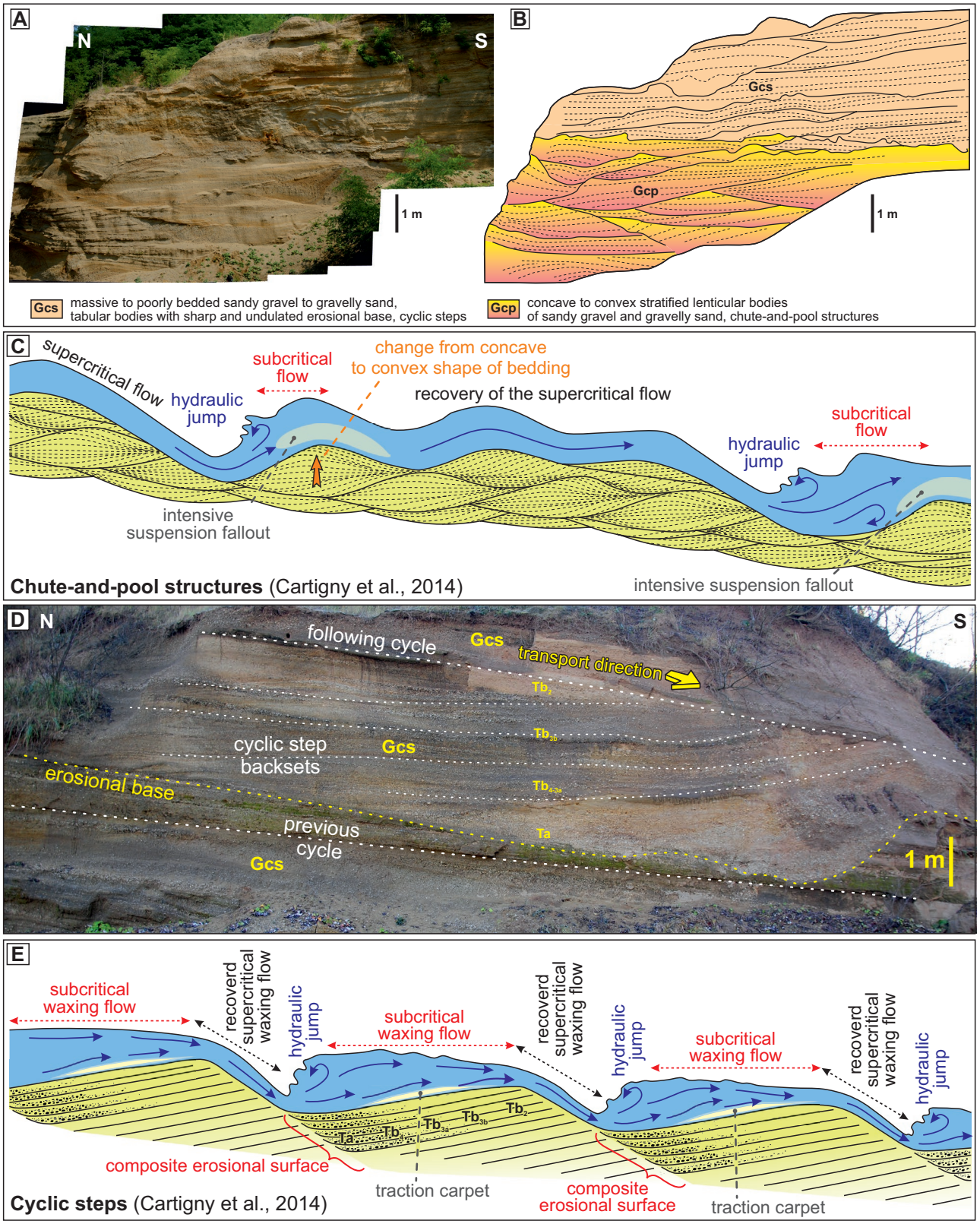

Fig. 4. Sedimentology of the Nemčiňany site: **A, B** — A scheme of facies distribution with chutes-and-pools in the lower portion and cyclic steps in the latter one. **C** — A conceptual model of the origin of chute-and-pool bedforms according to Cartigny et al. (2014). **D** — An example of the appearance of the cyclic steps bedform. The facies indexes according to Postma and Cartigny (2014). **E** — A conceptual model of origin of cyclic steps according to Cartigny et al. (2014). Suppl. Figure S1 shows the topography of the quarry and location of the depicted outcrop walls. Site location in Fig. 1C.

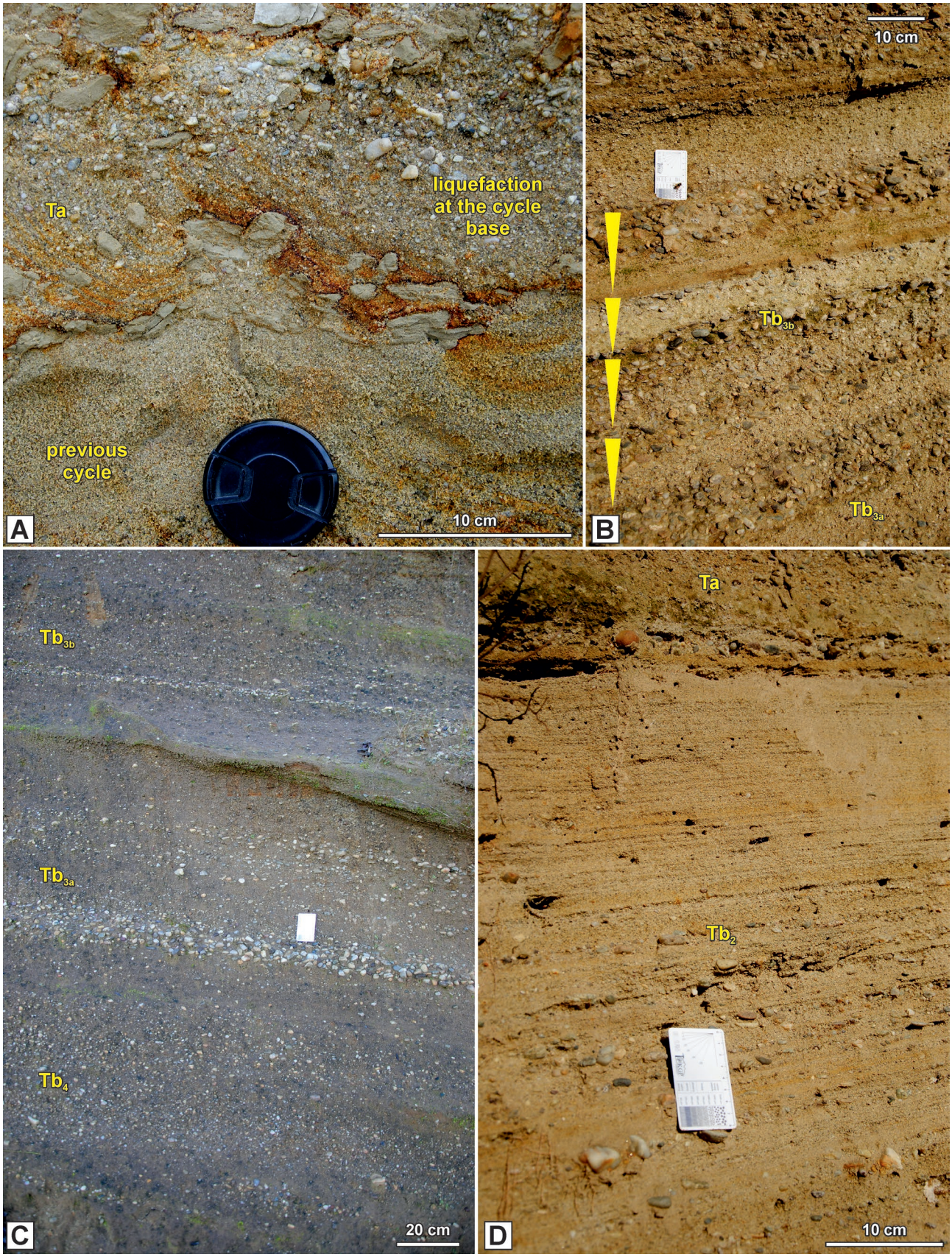

Fig. 5. Examples of the cyclic step facies observed at the Nemčiňany site and classified according to Postma & Cartigny (2014).

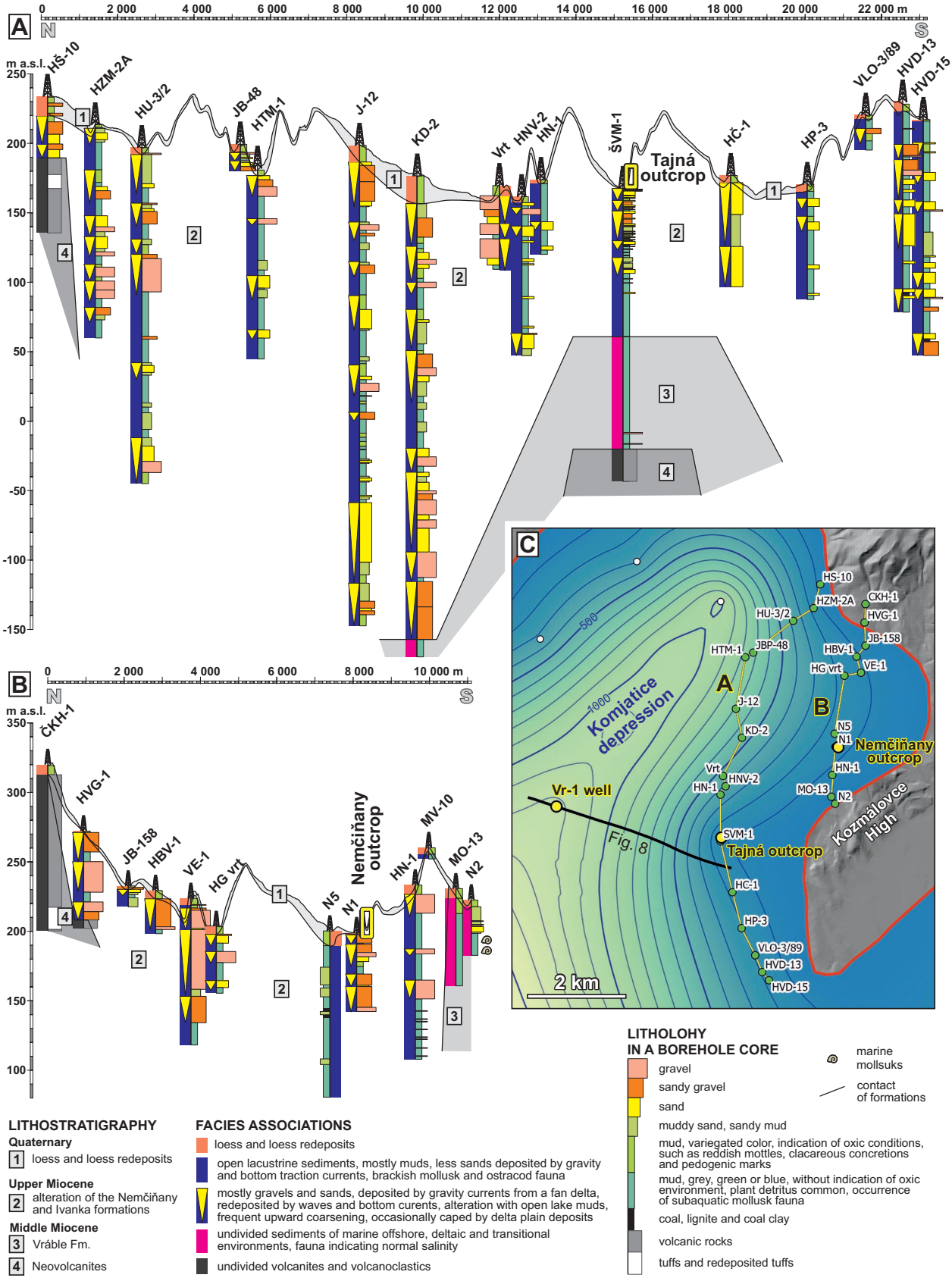

Fig. 6. Geological sections based on archival borehole profiles, showing the distribution of the Nemčiňany and Ivanka fms. on the eastern flank of the Komjatice depression. The borehole lithological logs are based on reports of geological surveys listed in Suppl. Table S1. Topography based on digital elevation model. See Fig. 1C for explanation of the insert map.

since the Middle Miocene successions are present on both sides. The Upper Miocene lacustrine–fan deltaic succession attains a thickness of up to 330 m in Fig. 6A and up to 140 m in Fig. 6B.

Authigenic $^{10}Be/^{9}Be$ dating

Five samples were analyzed from the overbank facies Fl and Fm (Figs. 2, 3). The obtained natural authigenic $^{10}Be/^{9}Be$ isotopic ratios show low variability in the range of 2.62 to 4.41×10^{-11} (Table 2). The analytical uncertainty reaches 3.5–4.0 %. The ages were calculated employing the floodplain initial ratio of $4.14\pm0.17\times10^{-9}$ (Šujan et al. 2016), corresponding to the depositional environment of the strata. The dating yielded ages in the range of 9.09–10.13 Ma. The dating uncertainty is 0.51–0.59 Ma (5.4–5.8 %), the ages overlap, forming a single population (Fig. 7). Hence, the weighted mean age of 9.60±0.26 Ma was calculated for the Tajná site using the KDX software by Spencer et al. (2017). Moreover, the weighted mean ages were calculated for the samples published in Šujan et al. (2016), taken at the Nemčiňany site and from the cores of the ŠVM-1 Tajná and Vráble-1 wells (Fig. 7). Suppl. Figure S4 illustrates the sampling positions at the Nemčiňany site. The original values are included in Suppl. Table S2. All sites appear as single populations , although ŠVM-1 exhibits two peaks in the age probability. The obtained values generally fall within the expected age range, roughly confined by the existence of Lake Pannon in the Komjatice depression of the Danube Basin between ~11.6–9.3 Ma (Sztanó et al. 2016; Šujan et al. 2016).

Discussion

A typical syn-rift to post-rift succession in the Pannonian Basin System

Distinct differences in lithology and depositional processes characterize transgressive and normal regressive deltaic systems within isolated epicontinental extensional basins. The former are typically locally-sourced fan deltas containing coarse sediment and associated with the rifting stage, while the latter consist of more remotely-sourced systems with extensive catchments and finer sediment grain size, often occurring in the post-rift stage (Evans 1988; Frostick & Reid 1989; Scholz et al. 1990; Allen & Allen 2013; Gobo et al. 2015; Matenco & Haq 2020; Fu et al. 2021; Song et al. 2022). Petrographic studies use changes in sediment provenance to establish the syn- and post-rift sequence boundaries, relying on the marked differences in sediment routing (Song et al. 2022; Wang et al. 2023).

Such a switch in the depositional settings is a characteristic feature in the Pannonian Basin System (Balázs et al. 2016, 2017). The basal Pannonian sandy-gravelly fan deltaic deposits are exposed at the Piusz Puszta site in Sopron–Eisenstadt Basin (Rosta 1993), whereas the Upper Miocene regressive deltaic clinoforms beneath the nearby Neusiedlersee exhibit a distinctly fine-grained lithology (Loisl et al. 2017). Similarly, in the Transdanubian Range area, the gravelly-sandy fan deltaic deposits of the Kálla Fm. are replaced by the normal regressive Újfalu Fm., which contains fine- to medium-grained sands sourced from the paleo-Danube (Csillag et al. 2010; Sztanó et al. 2013a). Analogously, variations between transgressive and normal regressive deltaic systems have been observed at the western tip of the Malé Karpaty Mts. between the Vienna and Danube basins by Šujan et al. (2021a), at the Mecsek Mts. in the central PBS by Budai et al. (2019) and also north of the Apuseni Mts. in the eastern PBS by Bartha et al. (2022). While not genetically a part of the PBS, the Vienna Basin demonstrates a similar pattern, with coarse-grained Hollabrun–Mistelbach Fm. underlying offshore Pannonian muds, all subsequently overlain by finer-grained deposits of the regressive paleo-Danube delta (Harzhauser et al. 2003, 2004; Nehyba & Roetzel 2004).

In addition to the evident lithological and provenance changes in the upward transition from syn-rift to post-rift succession, the described Pannonian syn-rift systems share a common feature in their relatively brief depositional period, typically lasting less than 1 Myr. Shortly after their initiation, the local sediment supply was outpaced by an increased accommodation rate, triggered by a relative rise in water level of Lake Pannon.

Nemčiňany Fm. – rifting to post-rift fan delta deposition induced by the paleo-Hron sediment supply

The authigenic $^{10}Be/^{9}Be$ dating age difference between the Nemčiňany and Tajná sites implies that the Nemčiňany Fm. depositional system persisted for at least 2 Myr.

Table 2: Concentrations of ^{9}Be and ^{10}Be, $^{10}Be/^{9}Be$ ratios and calculated ages for the analysed samples. Uncertainties are 1σ. Concentrations of ^{10}Be are corrected for the $^{10}Be/^{9}Be$ ratio of a single processing blank with the value of 3.88×10^{-15}.

ID	^{9}Be (at × g^{-1}) × 10^{16}	AMS $^{10}Be/^{9}Be$ (× 10^{-14})	^{10}Be (at × g^{-1}) × 10^{6}	Natural $^{10}Be/^{9}Be$ (× 10^{-11})	Age (Ma)	Weighted mean age (Ma)
Tajna-1	7.519 ± 0.150	7.840 ± 0.239	2.265 ± 0.070	3.012 ± 0.111	9.851 ± 0.549	
Tajna-2	7.996 ± 0.160	11.245 ± 0.346	3.300 ± 0.102	4.127 ± 0.152	9.221 ± 0.514	
Tajna-3	16.458 ± 0.329	16.281 ± 0.465	4.838 ± 0.139	2.940 ± 0.103	9.900 ± 0.539	9.600 ± 0.240
Tajna-4	9.746 ± 0.195	14.517 ± 0.452	4.296 ± 0.135	4.407 ± 0.164	9.090 ± 0.508	
Tajna-5	18.458 ± 0.369	16.263 ± 0.564	4.836 ± 0.168	2.620 ± 0.105	10.130 ± 0.586	

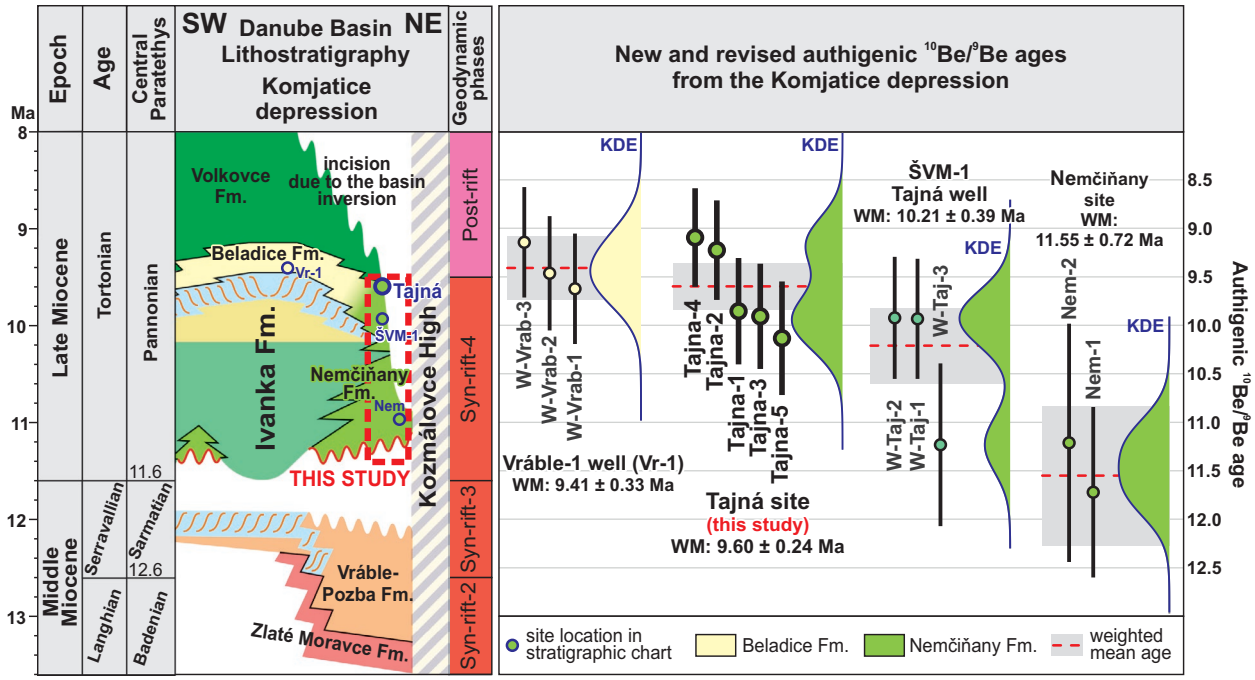

Fig. 7. Authigenic $^{10}Be/^{9}Be$ dating results and their stratigraphic context. Ages for the Vráble-1 well, ŠVM-1 Tajná well and the Nemčiňany outcrop are from Šujan et al. (2016). Weighted mean ages (WM) and Kernel Density Estimation (KDE) are established using the KDX software by Spencer et al. (2017), with 1σ as uncertainties. See Fig. 1D for the stratigraphic chart explanations.

The Nemčiňany site exposes fan delta foresets that entered the early Lake Pannon, as indicated by the presence of brackish-water mollusks *Congeria subglobosa* and *Congeria partschi* (Brestenská 1958). The formation shows a relatively homogeneous distribution of gravelly-sandy units of prograding fan delta lobes within the mud-dominated lacustrine Ivanka Fm. (Fig. 6), which implies a balanced accommodation to sediment supply ratio. The chaotic distribution of the fan-delta units likely mirrors stochastic character of autogenic delta lobe progradation (Van Dijk et al. 2009; Hajek & Straub 2017). The thickness of the muddy intervals that separate the fan delta units, reaching less than 50 meters, indicates a prevailing shallow lacustrine to sublittoral environment with a water depth of less than 100 meters, comparable to the Szák Fm. in the Transdanubian Range area (Cziczer et al. 2009).

The sedimentological interpretation of the Nemčiňany Formation presented in this study generally aligns with the assumptions made by Baráth & Kováč (1995). However, these authors did not fully comprehend the scale of the fan delta lobes, which most likely did not exceed a height of approximately 50 meters. Therefore, individual lobes had to reach spatial dimensions only a few hundred meters in size, much smaller in comparison with the published paleogeographic scenario. The model proposed by Baráth & Kováč (1995) incorporates a spatially fixed depositional system. However, the depositional record indicates repeated progradation of multiple small deltaic lobes, alternating with shallow lacustrine muds. On the other hand, the newly recognized upper flow regime bedforms have significantly enhanced the understanding of complex stratal geometries observed in the foreset facies association. Only delta foreset facies were observed at the Nemčiňany site, contrary to Baráth & Kováč (1995). The area of the Tajná site was considered as an anticlinal structure according to the interpretations of vintage reflection seismics (Holzbauer et al. 1969), in agreement with the geometry observed using the correlation of borehole profiles (Fig. 6). The thickness of the Upper Miocene succession increases towards the north from the Tajná site, perhaps indicating the existence of a syncline, where the major volume of the Nemčiňany Fm. accommodated. The open lacustrine Ivanka Fm., present below the Nemčiňany Fm. in the ŠVM-1 Tajná well, includes according to Kováč et al. (2008) fossils of the nannoplankton *Praenoelaerhabdus banatensis* with a biostratigraphic age range of ~11.3–10.7 Ma and a fossil mollusk *Lymnocardium schedelianum* having the biostratigraphic age constraints of ~11.0–10.3 Ma (Sztanó et al. 2016). It can be assumed that the fan delta depositional system prevailed in the northwestern part of the embayment shortly after the rifting, and later at ~10.5 Ma advanced towards the Tajná anticline, as evidenced by the Nemčiňany Fm. age of 10.21±0.39 Ma in the ŠVM-1 Tajná well.

The age of the Nemčiňany Fm. braidplain at the Tajná site reached 9.60±0.24 Ma and is very close to the age 9.41±0.33 Ma of the normal regressive deltaic Beladice Fm. in the Vráble-1 well (Fig. 7). A set of correlative Upper Miocene clinoforms appears between these sites (Fig. 8) (Šarinová et al. 2018; Rybár & Kotulová 2023), which reach

a thickness of >100 ms (two-way travel time) and could be considered as shelf-slopes (Patruno & Helland-Hansen 2018). Hence, the dated stratigraphic intervals at the Tajná site and Vráble-1 well represent a single depositional system, sourced from the Tajná braidplain towards the basin floor in the central Komjatice depression.

A question rises, why the Nemčiňany Fm. depositional system persisted for such long period. It occurred from the Late Miocene rifting until the post-rift stage and supplied the regressive progradational facies stacking pattern, despite this scenario was not observed elsewhere in the PBS. The explanation is provided by the character of the river, which deposited the formation. The petrographic composition of the gravel from the Nemčiňany and Tajná sites show generally a quarter formed by andesites and more than a half consisting of quartzite and less quartz according to Voštiarová (2013; Fig. 9A). The latter components include a variable fraction of carbonates (2–11 %), changing proportion of metamorphic rocks (9–17 %) and 0–5 % of granitoids. The Quaternary river terraces of the Hron river differ in the presence of rhyolite, which is absent in the Upper Miocene strata, and by a higher proportion of granitoids (Minaříková 1967; Vaškovský et al. 1979; Fig. 9B, C). Considering ca. 9 Myr of incision of the river network and denudation of rock complexes in the Western Carpathians, which separate the compared Upper Miocene and Quaternary sites, the representation of petrographic groups generally matches well. These observations support the previously published paleogeographic view of the paleo-Hron river supplying the Nemčiňany Fm. (Priechodská & Harčár 1988; Baráth & Kováč 1995; Kováč et al. 2006). The orientation of fan delta foreset progradation toward the west at the Nemčiňany site (Suppl. Fig. S2) further substantiates its connection to the paleo-Hron river as the source. The present-day Hron river represents a major stream of the Western Carpathians, draining almost 5500 km^2 of mountainous landscape, and entering the Danube Basin just on the margin of the study area (Fig. 10). The increased accommodation rate during the Lake Pannon flooding was therefore likely compensated by the high sediment supply of the paleo-Hron river delta, which continuously occupied the eastern flank of the Komjatice depression (Fig. 10A, B).

On the other hand, the shelf-slope progradation patterns in the Danube Basin do not include aggradational clinothem sets (Kováč et al. 2011; Sztanó et al. 2016; Magyar et al. 2020), which points to the lack of an increase in water level during normal regression (Sztanó et al. 2013b). Hence, the restricted

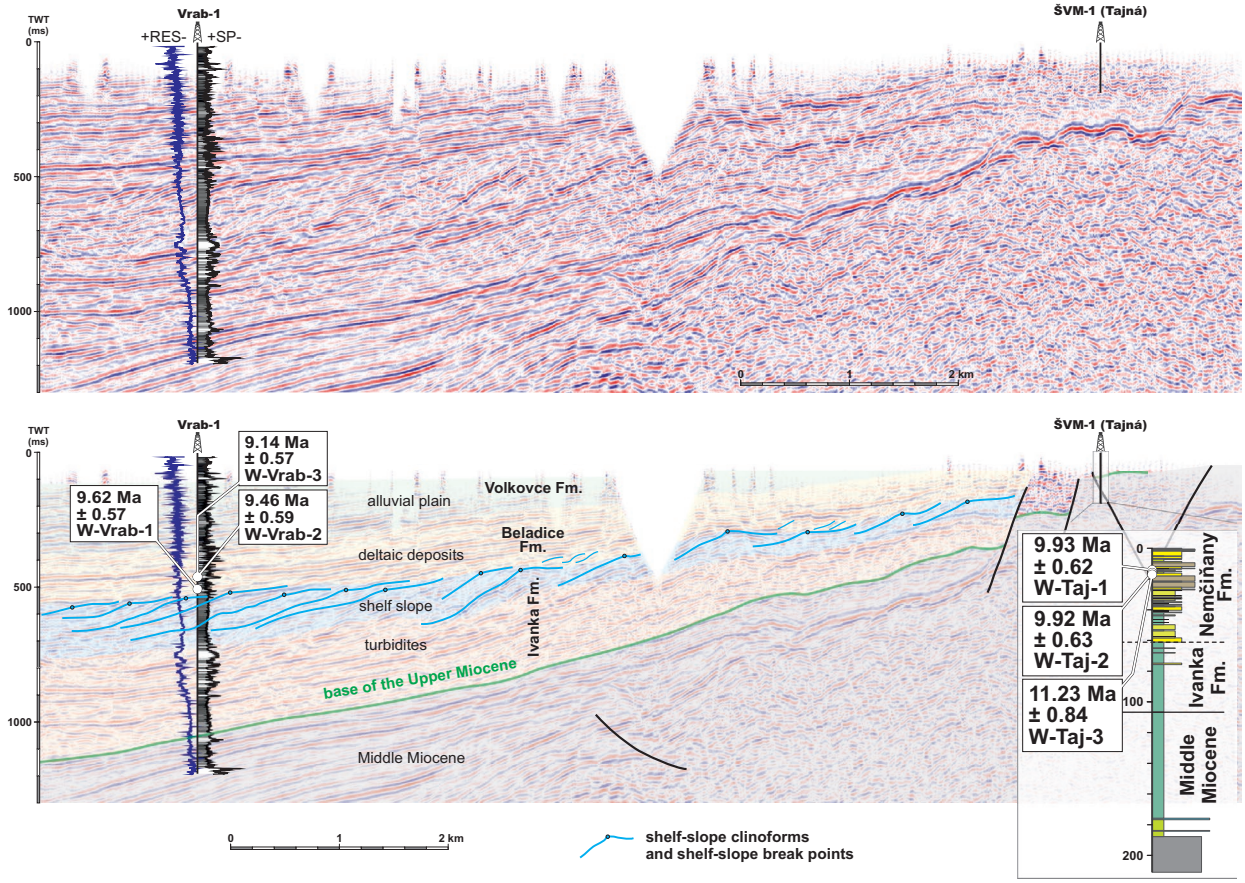

Fig. 8. Reflection seismic line 820/00, interpretation according to Rybár and Kotulová (2023), modified. Shelf-slope clinoforms *sensu* Patruno and Helland-Hansen (2018). Authigenic ^{10}Be/^{9}Be ages and well-logs of the Vráble-1 well from Šujan et al. (2016). Simplified profile of the ŠVM-1 Tajná well according to Kováč et al. (2008). Explanation of the lithological log in Fig. 6.

accommodation during the post-rift stage allowed the paleo-Hron deltaic system to form shelf-slopes and prograde across the Komjatice depression with a relatively unchanged sediment supply (Fig. 10C). The boreholes on the northwestern flank of the Komjatice depression (Mojmírovce well series; Fig. 10) indicate a minimal presence of gravels only at the base of the lacustrine Ivanka Formation (Čermák 1971, 1972). Consequently, the fan deltas sourced locally were overshadowed by the increased accommodation shortly after the onset of the Lake Pannon transgression. Only the wells located at the northeastern tip, near the Zlaté Moravce-1 well (ZM-1), show a more frequent occurrence of sandy-gravelly layers within the lacustrine succession. These layers likely represent the marginal part of the Nemčiňany depositional system (Fig. 10C). The paleo-Hron delta plain merged with the paleo-Danube system, which appeared in the area at ~9.3 Ma (Magyar et al. 2013).

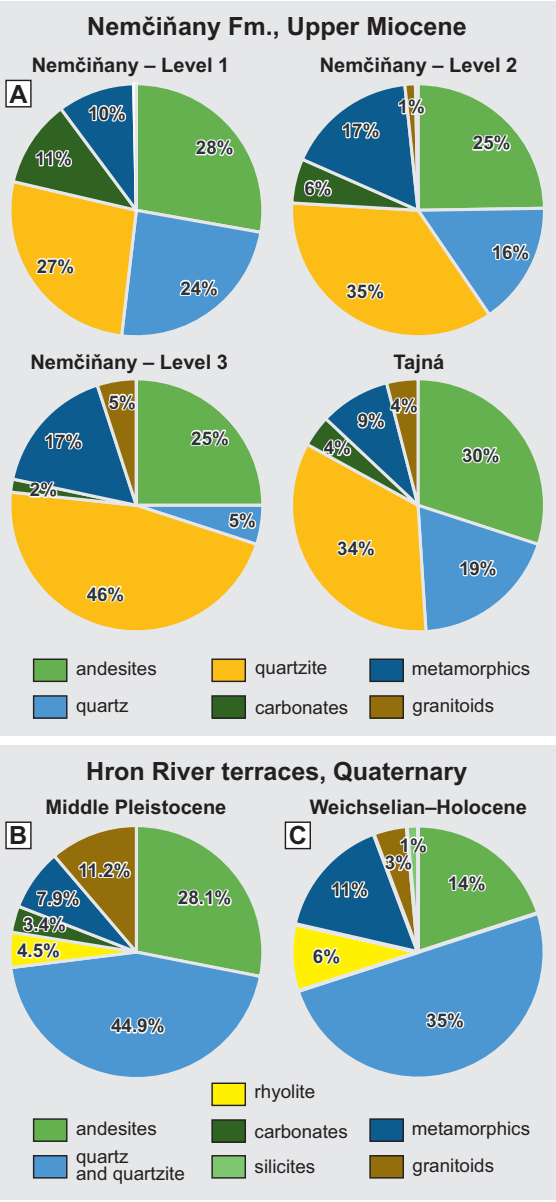

Fig. 9. A comparison of the petrographic composition of the Nemčiňany Fm. and the Quaternary deposits of the Hron River in the area of Hron Upland: **A** — Petrographic composition of gravel at the Nemčiňany and Tajná sites according to Voštiarová (2013). **B** — Petrographic composition of river terrace gravel at the Middle Pleistocene Nýrovce site according to Vaškovský et al. (1979). **C** — Petrographic composition of river terrace gravel at the Weicheslian–Holocene Štúrovo site according to Minaříková (1967).

The documented scenario has important implications for the analysis of the past evolution of basins, particularly when the preservation of a depositional record is scarce, and the temporal and spatial relationships of depositional systems are unclear. A general assumption of a change in depositional systems and sediment provenance is often used to trace the transition from syn-rift to post-rift (e.g., Barham & Kirkland 2020; He et al. 2020; Wang et al. 2023). However, our study demonstrates that the specific settings of a basin margin along exposed mountains may lead to persistent depositional system characteristics without significant change, even as geodynamic stages shift.

Conclusions

This study presents a sedimentological and stratigraphic analysis of the Nemčiňany Formation, integrated with the authigenic $^{10}Be/^{9}Be$ dating, aiming to provide a detailed reconstruction of the temporal and spatial evolution of the Late Miocene fan deltaic depositional system in the eastern Danube Basin. The Nemčiňany outcrop reveals a fan delta foreset facies association, which includes upper flow regime bedforms deposited at ~11.5 Ma. At the Tajná site, a delta topset braidplain facies association was interpreted, dating back to ~9.6 Ma. Consequently, it is demonstrated that the Nemčiňany Formation fan deltas accumulated during the syn-rift stage and persisted in a steady sediment supply to accommodation rate settings until the post-rift stage of the Danube Basin. The long-living nature of the fan deltaic depositional system, a phenomenon uncommon in the Pannonian Basin System, is attributed to the substantial sediment influx from the paleo-Hron River, one of the major streams of the Western Carpathians. A relative decrease in accommodation rates during the post-rift stage caused progradation of the Nemčiňany fan deltas across the deep-water depocenter between ~9.6–9.4 Ma, forming shelf-slope clinoforms. Consequently, integration with the paleo-Danube depositional system appeared. The stable sedimentary environment and provenance settings defy the conventional understanding of the depositional record during the syn-rift to post-rift transition and the associated transgressive to regressive successions in isolated epicontinental basins.

Acknowledgements: The study was supported by the Slovak Research and Development Agency (APVV) under contracts Nos. APVV-16-0121, APVV-20-0120 and APVV-21-0281, and by the Scientific Grant Agency of the Ministry of Educa-

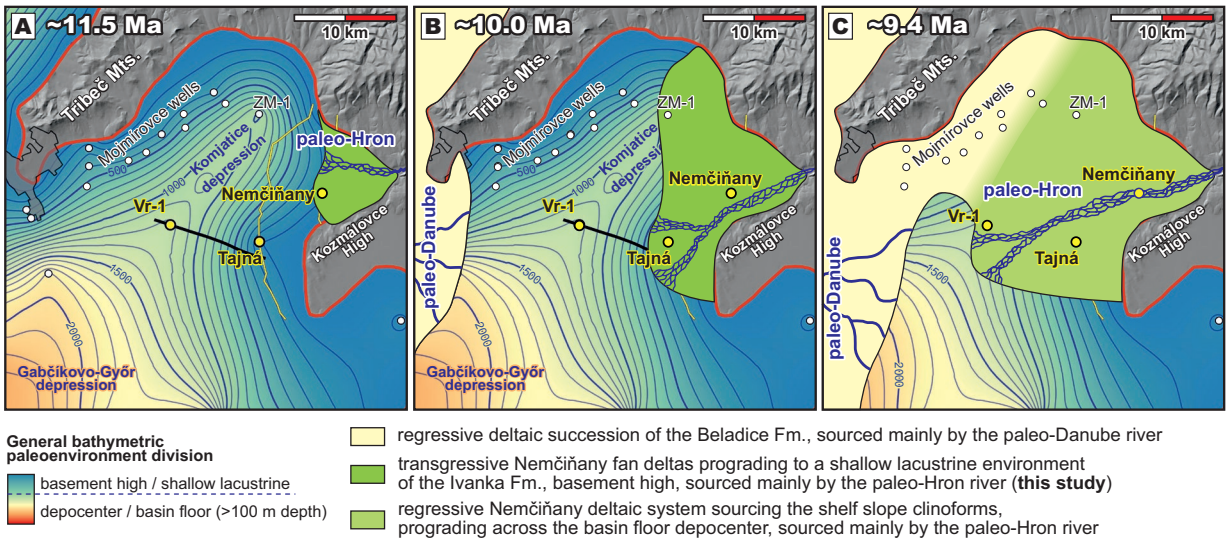

Fig. 10. Inferred evolution of the transgressive to regressive deltaic systems entering Lake Pannon during the Late Miocene in the eastern Danube Basin. The paleo-Hron and paleo-Danube deltaic systems rhythmically prograded into shallow water environment and formed parasequences in the colored areas. Mojmírovce wells indicate a selection from the well series, which penetrated the base of the Upper Miocene succession or close to it and is relevant for the distribution of the Nemčiňany Fm. (according to Čermák 1971, 1972).

tion, Science, Research and Sport of the Slovak Republic and the Slovak Academy of Sciences (VEGA) under the contract No. 1/0533/21. The free availability of the Lidar DEM data owned by the Geodesy, Cartography and Cadaster Authority of the Slovak Republic (ÚGKK SR) and distributed by the Geodetic and Cartographic Institute, Bratislava (GKÚ) is acknowledged with gratitude. The ASTER AMS national facility (CEREGE, Aix-en-Provence, France) is supported by the INSU/CNRS, the ANR through the "Projets thématiques d'excellence" program for the "Equipements d'excellence" ASTER-CEREGE action, and IRD. We express our gratitude to the reviewers Stephanie Neuhuber and Ľubomír Sliva for their constructive feedback and helpful suggestions that have substantially improved the original manuscript.

References

Aherwar K., Šujan M., Šarinová K., Braucher R., de Leeuw A., Chyba A. & AsterTeam 2021: Applicability of the authigenic $^{10}Be/^{9}Be$ dating to deltaic deposits: Preliminary results from the Slanicul de Buzau section, Pliocene, Romania. *EGU General Assembly 2021, online, 19–30 Apr 2021, EGU21-13808.* https://doi.org/10.5194/egusphere-egu21-13808

Allen J.R.L. 1982: Sedimentary Structures: Their Character and Physical Basis. *Elsevier, Amsterdam*, 1–663.

Allen P.A. & Allen J.R. 2013: Basin Analysis: Principles and Application to Petroleum Play Assessment, 3rd Edition. *Wiley-Blackwell*, Oxford, 1–619.

Arnold M., Merchel S., Bourlès D.L., Braucher R., Benedetti L., Finkel R.C., Aumaître G., Gottdang A. & Klein M. 2010: The French accelerator mass spectrometry facility ASTER: Improved performance and developments. *Nuclear Instruments and Methods in Physics Research Section B: Beam Interactions with Materials and Atoms* 268, 1954–1959. https://doi.org/10.1016/j.nimb.2010.02.107

Aslan A. & Autin W.J. 1999: Evolution of the Holocene Mississippi River floodplain, Ferriday, Louisiana: Insights on the origin of fine-grained floodplains. *Journal of Sedimentary Research* 69, 800–815. https://doi.org/10.1306/D4268A95-2B26-11D7-8648000102C1865D

Baas J.H., Best J.L. & Peakall J. 2016: Predicting bedforms and primary current stratification in cohesive mixtures of mud and sand. *Journal of the Geological Society* 173, 12–45. https://doi.org/10.1144/jgs2015-024

Balázs A., Matenco L., Magyar I., Horváth F. & Cloetingh S. 2016: The link between tectonics and sedimentation in back-arc basins: New genetic constraints from the analysis of the Pannonian Basin. *Tectonics* 35, 1526–1559. https://doi.org/10.1002/2015tc004109

Balázs A., Burov E., Matenco L., Vogt K., Francois T. & Cloetingh S. 2017: Symmetry during the syn- and post-rift evolution of extensional back-arc basins: The role of inherited orogenic structures. *Earth and Planetary Science Letters* 462, 86–98. https://doi.org/10.1016/j.epsl.2017.01.015

Balázs A., Magyar I., Matenco L., Sztanó O., Tőkés L. & Horváth F. 2018: Morphology of a large paleo-lake: Analysis of compaction in the Miocene-Quaternary Pannonian Basin. *Global and Planetary Change* 171, 134–147. https://doi.org/10.1016/j.gloplacha.2017.10.012

Baráth I. & Kováč M. 1995: Sedimentology and paleogeography of the Pliocene Hron river delta in the Komjatice depression (Danube Basin). *Mineralia Slovaca* 27, 236–242.

Barham M. & Kirkland C.L. 2020: Changing of the guards: Detrital zircon provenance tracking sedimentological reorganization of a post-Gondwanan rift margin. *Basin Research* 32, 854–874. https://doi.org/10.1111/bre.12403

Bartha I.R., Botka D., Csoma V., Katona L.T., Tóth E., Magyar I., Silye L. & Sztanó O. 2022: From marginal outcrops to basin interior: a new perspective on the sedimentary evolution of the eastern Pannonian Basin. *International Journal of Earth Sciences* 111, 335–357. https://doi.org/10.1007/s00531-021-02117-6

Boothroyd J.C. & Ashley G.M. 1975: Processes, Bar Morphology, and Sedimentary Structures on Braided Outwash Fans, North-

eastern Gulf of Alaska. In: A.V. Jopling & B.C. McDonald (Eds.): Glaciofluvial and Glaciolacustrine Sedimentation. *SEPM Society for Sedimentary Geology*, 193–222.

Bourlès D., Raisbeck G.M. & Yiou F. 1989: ^{10}Be and ^{9}Be in marine sediments and their potential for dating. *Geochimica et Cosmochimica Acta* 53, 443–452. https://doi.org/10.1016/0016-7037(89)90395-5

Brenna A., Surian N., Ghinassi M. & Marchi L. 2020: Sediment–water flows in mountain streams: Recognition and classification based on field evidence. *Geomorphology* 371, 107413. https://doi.org/10.1016/j.geomorph.2020.107413

Brestenská E. 1958: Zpráva o geologickom mapovaní západnej časti listu Sv. Beňadik – 4661/3. Manuscript, Geofond Nr. 1430, *State Geological Istitute of Dionýz Štúr*, Bratislava, 1–15. Available online at: https://da.geology.sk/navigator/?desktop=Public

Bridge J.S. & Lunt I.A. 2006: Depositional models of braided rivers. In: G.H. Sambrook Smith, J.L. Best, C.S. Bristow & G.E. Petts (Eds.): Braided Rivers: Process, Deposits, Ecology and Management. *International Association of Sedimentologists Special Publication, Wiley-Blackwell*, Oxford, 1–396.

Brown E.T., Edmond J.M., Raisbeck G.M., Bourlès D.L., Yiou F. & Measures C.I. 1992: Beryllium isotope geochemistry in tropical river basins. *Geochimica et Cosmochimica Acta* 56, 1607–1624. https://doi.org/10.1016/0016-7037(92)90228-B

Budai S., Sebe K., Nagy G., Magyar I. & Sztanó O. 2019: Interplay of sediment supply and lake-level changes on the margin of an intrabasinal basement high in the Late Miocene Lake Pannon (Mecsek Mts., Hungary). *International Journal of Earth Sciences* 108, 2001–2019. https://doi.org/10.1007/s00531-019-01745-3

Burns B.A., Heller P.L., Marzo M. & Paola C. 1997: Fluvial response in a sequence stratigraphic framework; example from the Montserrat fan delta, Spain. *Journal of Sedimentary Research* 67, 311–321. https://doi.org/10.1306/d426855e-2b26-11d7-8648000102c1865d

Campo B., Amorosi A. & Bruno L. 2016: Contrasting alluvial architecture of Late Pleistocene and Holocene deposits along a 120-km transect from the central Po Plain (northern Italy). *Sedimentary Geology* 341, 265–275. https://doi.org/10.1016/j.sedgeo.2016.04.013

Cartigny M.J.B., Ventra D., Postma G. & van Den Berg J.H. 2014: Morphodynamics and sedimentary structures of bedforms under supercritical-flow conditions: New insights from flume experiments. *Sedimentology* 61, 712–748. https://doi.org/10.1111/sed.12076

Casalbore D., Chiocci F.L., Scarascia Mugnozza G., Tommasi P. & Sposato A. 2011: Flash-flood hyperpycnal flows generating shallow-water landslides at Fiumara mouths in Western Messina Strait (Italy). *Marine Geophysical Research* 32, 257–271. https://doi.org/10.1007/s11001-011-9128-y

Catuneanu O. 2006: Principles of Sequence Stratigraphy. *Elsevier*, Amsterdam, 1–375.

Čermák D. 1971: Komjatická depresia – stredne hlboký štruktúrny prieskum, prieskum živíc, výročná správa za rok 1971. Manuscript, Geofond Nr. 29258, *Nafta*, Gbely, 1–14. Available onlie at: https://da.geology.sk/navigator/?desktop=Public

Čermák D. 1972: Stredne hlboký štruktúrny prieskum komjatickej depresie, výročná správa za rok 1972, náplň úlohy (suroviny): prieskum živíc. Manuscript, Geofond Nr. 29362, *Nafta*, Gbely, 1–11. Available onlie at: https://da.geology.sk/navigator/?desktop=Public

Chmeleff J., von Blanckenburg F., Kossert K. & Jakob D. 2010: Determination of the ^{10}Be half-life by multicollector ICP-MS and liquid scintillation counting. *Nuclear Instruments and Methods in Physics Research, Section B: Beam Interactions with Materials and Atoms* 268, 192–199. https://doi.org/10.1016/j.nimb.2009.09.012

Church M. & Jakob M. 2020: What Is a Debris Flood? *Water Resources Research* 56, e2020WR027144. https://doi.org/10.1029/2020WR027144

Cloetingh S., Ziegler P.A., Beekman F., Burov E.B., Garcia-Castellanos D., Matenco L. & Schubert G. 2015: 6.12 – Tectonic Models for the Evolution of Sedimentary Basins, Treatise on Geophysics (Second Edition). *Elsevier*, Oxford, 513–592.

Cloetingh S., Sternai P., Koptev A., Ehlers T.A., Gerya T., Kovács I., Oerlemans J., Beekman F., Lavallée Y., Dingwell D., Békési E., Porkolàb K., Tesauro M., Lavecchia A., Botsyun S., Muller V., Roure F., Serpelloni E., Matenco L., Castelltort S., Giovannelli D., Brovarone A.V., Malaspina N., Coletti G., Valla P. & Limberger J. 2023: Coupled surface to deep Earth processes: Perspectives from TOPO-EUROPE with an emphasis on climate- and energy-related societal challenges. *Global and Planetary Change* 226, 104140. https://doi.org/10.1016/j.gloplacha.2023.104140

Csillag G., Sztanó O., Magyar I. & Hámori Z. 2010: Stratigraphy of the Kálla Gravel in Tapolca Basin based on multi-electrode probing and well data. *Foldtani Kozlony* 140, 183–196.

Cziczer I., Magyar I., Pipík R., Böhme M., Ćorić S., Bakrač K., Sütó-Szentai M., Lantos M., Babinszki E. & Müller P. 2009: Life in the sublittoral zone of long-lived Lake Pannon: Paleontological analysis of the Upper Miocene Szák Formation, Hungary. *International Journal of Earth Sciences* 98, 1741–1766. https://doi.org/10.1007/s00531-008-0322-3

Evans A.L. 1988: Neogene tectonic and stratigraphic events in the Gulf of Suez rift area, Egypt. *Tectonophysics* 153, 235–247. https://doi.org/10.1016/0040-1951(88)90018-2

Fricke A.T., Sheets B.A., Nittrouer C.A., Allison M.A. & Ogston A.S. 2015: An Examination of Froude-Supercritical Flows and Cyclic Steps On A Subaqueous Lacustrine Delta, Lake Chelan, Washington, U.S.A. *Journal of Sedimentary Research* 85, 754–767. https://doi.org/10.2110/jsr.2015.48

Frostick L.E. & Reid I. 1989: Is structure the main control of river drainage and sedimentation in rifts? *Journal of African Earth Sciences* 8, 165–182. https://doi.org/10.1016/S0899-5362(89)80022-3

Fu C., Li S., Li S. & Xu J. 2021: Spatial and temporal variability of sediment infilling and episodic rifting in the North Pearl River Mouth Basin, South China Sea. *Journal of Asian Earth Sciences* 211, 104702. https://doi.org/10.1016/j.jseaes.2021.104702

Gobo K., Ghinassi M. & Nemec W. 2015: Gilbert-type deltas recording short-term base-level changes: Delta-brink morphodynamics and related foreset facies. *Sedimentology* 62, 1923–1949. https://doi.org/10.1111/sed.12212

Hage S., Cartigny M.J.B., Clare M.A., Sumner E.J., Vendettuoli D., Clarke J.E.H., Hubbard S.M., Talling P.J., Gwyn Lintern D., Stacey C.D., Englert R.G., Vardy M.E., Hunt J.E., Yokokawa M., Parsons D.R., Hizzett J.L., Azpiroz-Zabala M. & Vellinga A.J. 2018: How to recognize crescentic bedforms formed by supercritical turbidity currents in the geologic record: Insights from active submarine channels. *Geology* 46, 563–566. https://doi.org/10.1130/G40095.1

Hajek E.A. & Straub K.M. 2017: Autogenic Sedimentation in Clastic Stratigraphy. *Annual Review of Earth and Planetary Sciences* 45, 681–709.

Harzhauser M. & Mandic O. 2008: Neogene lake systems of Central and South-Eastern Europe: Faunal diversity, gradients and interrelations. *Palaeogeography, Palaeoclimatology, Palaeoecology* 260, 417–434. https://doi.org/10.1016/j.palaeo.2007.12.013

Harzhauser M., Kovar-Eder J., Nehyba S., Strobitzer-Hermann M., Schwarz J., Wojcicki J. & Zorn I. 2003: An Early Pannonian (Late Miocene) transgression in the Northern Vienna Basin. The paleoecological feedback. *Geologica Carpathica* 54, 41–52.

Harzhauser M., Daxner-Hock G. & Piller E.W. 2004: An integrated stratigraphy of the Pannonian (Late Miocene) in the Vienna Basin. *Austrian Journal of Earth Sciences* 95–96, 6–19.

He J., Garzanti E., Cao L. & Wang H. 2020: The zircon story of the Pearl River (China) from Cretaceous to present. *Earth-Science Reviews* 201, 103078. https://doi.org/10.1016/j.earscirev.2019.103078

Holzbauer K., Beinhauerová M. & Paulík J. 1969: Správa o refrakčno-seizmickom prieskume Podunajskej nížiny v roku 1968, oblasť Komjatickej depresie, česky. Manuskript, Geofond Nr. 21267. *Ústav užité geofyziky*, Brno, 1–43.

Horváth F. 1993: Towards a mechanical model for the formation of the Pannonian basin. *Tectonophysics* 226, 333–357. https://doi.org/10.1016/0040-1951(93)90126-5

Horvath F. & Cloetingh S. 1996: Stress-induced late-stage subsidence anomalies in the Pannonian basin. *Tectonophysics* 266, 287–300. https://doi.org/10.1016/s0040-1951(96)00194-1

Horváth F., Musitz B., Balázs A., Végh A., Uhrin A., Nádor A., Koroknai B., Pap N., Tóth T. & Wórum G. 2015: Evolution of the Pannonian basin and its geothermal resources. *Geothermics* 53, 328–352. https://doi.org/10.1016/j.geothermics.2014.07.009

Joniak P., Šujan M., Fordinál K., Braucher R., Rybár S., Kováčová M., Kováč M., Aumaître G., Bourlès D.L. & Keddadouche K. 2020: The age and paleoenvironment of a late Miocene floodplain alongside Lake Pannon: Rodent and mollusk biostratigraphy coupled with authigenic $^{10}Be/^{9}Be$ dating in the northern Danube Basin of Slovakia. *Palaeogeography, Palaeoclimatology, Palaeoecology* 538, 109482. https://doi.org/10.1016/j.palaeo.2019.109482

Kelder N.A., Sant K., Dekkers M.J., Magyar I., van Dijk G.A., Lathouwers Y.Z., Sztanó O. & Krijgsman W. 2018: Paleomagnetism in Lake Pannon: Problems, Pitfalls, and Progress in Using Iron Sulfides for Magnetostratigraphy. *Geochemistry, Geophysics, Geosystems* 19, 3405–3429. https://doi.org/10.1029/2018GC007673

Kong W.Y., Zhou L.P. & AsterTeam 2021: Tracing Water Masses and Assessing Boundary Scavenging Intensity With Beryllium Isotopes in the Northern South China Sea. *Journal of Geophysical Research: Oceans* 126, e2021JC017236. https://doi.org/10.1029/2021JC017236

Korschinek G., Bergmaier A., Faestermann T., Gerstmann U.C., Knie K., Rugel G., Wallner A., Dillmann I., Dollinger G., von Gostomski C.L., Kossert K., Maiti M., Poutivtsev M. & Remmert A. 2010: A new value for the half-life of Be-10 by Heavy-Ion Elastic Recoil Detection and liquid scintillation counting. *Nuclear Instruments & Methods in Physics Research Section B-Beam Interactions with Materials and Atoms* 268, 187–191. https://doi.org/10.1016/j.nimb.2009.09.020

Kováč M., Baráth I., Fordinál K., Grigorovich A.S., Halásová E., Hudáčková N., Joniak P., Sabol M., Slamková M., Sliva Ľ. & Vojtko R. 2006: Late Miocene to Early Pliocene sedimentary environments and climatic changes in the Alpine–Carpathian–Pannonian junction area: A case study from the Danube Basin northern margin (Slovakia). *Palaeogeography, Palaeoclimatology, Palaeoecology* 238, 32–52. https://doi.org/10.1016/j.palaeo.2006.03.015

Kováč M., Andrejeva-Grigorovič A., Baráth I., Beláčková K., Fordinál K., Halásová E., Hók J., Hudáčková N., Chalupová B., Kováčová M., Sliva Ľ. & Šujan M. 2008: Litologické, sedimentologické a biostratigrafické vyhodnotenie vrtu ŠVM-1 Tajná. *Geologické práce, Správy* 114, 51–84 (in Slovak with English abstract).

Kováč M., Synak R., Fordinál K., Joniak P., Tóth C., Vojtko R., Nagy A., Baráth I., Maglay J. & Minár J. 2011: Late Miocene and Pliocene history of the Danube Basin: Inferred from development of depositional systems and timing of sedimentary facies changes. *Geologica Carpathica* 62, 519–534. https://doi.org/10.2478/v10096-011-0037-4

Kováč M., Márton E., Oszczypko N., Vojtko R., Hók J., Králiková S., Plašienka D., Klučiar T., Hudáčková N. & Oszczypko-Clowes M. 2017: Neogene palaeogeography and basin evolution of the Western Carpathians, Northern Pannonian domain and adjoining areas. *Global and Planetary Change* 155, 133–154. https://doi.org/10.1016/j.gloplacha.2017.07.004

Kováč M., Halásová E., Hudáčková N., Holcová K., Hyžný M., Jamrich M. & Ruman A. 2018: Towards better correlation of the Central Paratethys regional time scale with the standard geological time scale of the Miocene Epoch. *Geologica Carpathica* 69, 283–300. https://doi.org/10.1515/geoca-2018-0017

Kováč P. & Hók J. 1993: The Central Slovak Fault System – the field evidence of a strike slip. *Geologica Carpathica* 44, 155–159.

Langereis G., Krijgsman W., Muttoni G. & Menning M. 2010: Magnetostratigraphy – concepts, definitions, and applications. *Newsletters on Stratigraphy* 43, 207–233. https://doi.org/10.1127/0078-0421/2010/0043-0207

Lankreijer A., Kováč M., Cloetingh S., Pitoňák P., Hlôška M. & Biermann C. 1995: Quantitative subsidence analysis and forward modelling of the Vienna and Danube basins: thin-skinned versus thick-skinned extension. *Tectonophysics* 252, 433–451. https://doi.org/10.1016/0040-1951(95)00099-2

Lebatard A.E., Bourlès D.L., Duringer P., Jolivet M., Braucher R., Carcaillet J., Schuster M., Arnaud N., Monié P., Lihoreau F., Likius A., Mackaye H.T., Vignaud P. & Brunet M. 2008: Cosmogenic nuclide dating of Sahelanthropus tchadensis and Australopithecus bahrelghazali: Mio-Pliocene hominids from Chad. *Proceedings of the National Academy of Sciences of the United States of America* 105, 3226–3231. https://doi.org/10.1073/pnas.0708015105

Leclair S.F. & Bridge J.S. 2001: Quantitative interpretation of sedimentary structures formed by river dunes. *Journal of Sedimentary Research* 71, 713–716.

Lirer F., Harzhauser M., Pelosi N., Piller W.E., Schmid H.P. & Sprovieri M. 2009: Astronomically forced teleconnection between Paratethyan and Mediterranean sediments during the Middle and Late Miocene. *Palaeogeography, Palaeoclimatology, Palaeoecology* 275, 1–13. https://doi.org/10.1016/j.palaeo.2009.01.006

Loisl J., Tari G., Draganits E., Zámolyi A. & Gjerazi I. 2017: High-resolution seismic reflection data acquisition and interpretation, Lake Neusiedl, Austria, NW Pannonian Basin. *Interpretation* 6. https://doi.org/10.1190/int-2017-0086.1

Lojka R., Sidorinová T., Rosenau N.A. & Strnad L. 2016: Architecture, paleosols and cyclicity of the middle-late pennsylvanian proximal fluvial system (Nýřany member, Pilsen Basin, Czech republic). *Bulletin of Geosciences* 91, 111–140. https://doi.org/10.3140/bull.geosci.1509

Longhitano S.G. 2008: Sedimentary facies and sequence stratigraphy of coarse-grained Gilbert-type deltas within the Pliocene thrust-top Potenza Basin (Southern Apennines, Italy). *Sedimentary Geology* 210, 87–110. https://doi.org/10.1016/j.sedgeo.2008.07.004

Magyar I. 2021: Chronostratigraphy of clinothem-filled non-marine basins: Dating the Pannonian Stage. *Global and Planetary Change* 205, 103609. https://doi.org/10.1016/j.gloplacha.2021.103609

Magyar I., Geary D.H. & Müller P. 1999: Paleogeographic evolution of the Late Miocene Lake Pannon in Central Europe. *Palaeogeography, Palaeoclimatology, Palaeoecology* 147, 151–167. https://doi.org/10.1016/S0031-0182(98)00155-2

Magyar I., Radivojevic D., Sztano O., Synak R., Ujszaszi K. & Pocsik M. 2013: Progradation of the paleo-Danube shelf margin across

the Pannonian Basin during the Late Miocene and Early Pliocene. *Global and Planetary Change* 103, 168–173. https://doi.org/10.1016/j.gloplacha.2012.06.007

Magyar I., Krezsek C. & Tari G. 2020: Clinoforms as paleogeographic tools: Development of the Danube catchment above the deep Paratethyan basins in Central and Southeast Europe. *Basin Research* 32, 320–331. https://doi.org/10.1111/bre.12401

Manville V. & White J.D.L. 2003: Incipient granular mass flows at the base of sediment-laden floods, and the roles of flow competence and flow capacity in the deposition of stratified bouldery sands. *Sedimentary Geology* 155, 157–173. https://doi.org/10.1016/S0037-0738(02)00294-4

Martini I., Ambrosetti E. & Sandrelli F. 2017: The role of sediment supply in large-scale stratigraphic architecture of ancient Gilbert-type deltas (Pliocene Siena-Radicofani Basin, Italy). *Sedimentary Geology* 350, 23–41. https://doi.org/10.1016/j.sedgeo.2017.01.006

Matenco L.C. & Haq B.U. 2020: Multi-scale depositional successions in tectonic settings. *Earth-Science Reviews* 200, 102991. https://doi.org/10.1016/j.earscirev.2019.102991

Measures C.I. & Edmond J.M. 1983: The geochemical cycle of ^{9}Be: a reconnaissance. *Earth and Planetary Science Letters* 66, 101–110.

Merchel S. & Herpers U. 1999: An Update on Radiochemical Separation Techniques for the Determination of Long-Lived Radionuclides via Accelerator Mass Spectrometry. *Radiochimica Acta* 84, 215–220. https://doi.org/10.1524/ract.1999.84.4.215

Minaříková D. 1967: Sedimentárno-petrografický výskum kvartérnych sedimentov územia medzi Komárnom a Štúrovom, dielčia záverečná správa za roky 1959–1966. Názov úlohy v perspektívnom pláne: Sedimentárno-petrografický výskum kvartérnych sedimentov Západných Karpát, česky. Manuscript, Geofond Nr. 19907, *State Geological Survey of Dionýz Štúr,* Bratislava, 1–70. Available online at: https://da.geology.sk/navigator/?desktop=Public

Nehyba S. & Roetzel R. 2004: The Hollabrunn-Mistelbach Formation (Upper Miocene, Pannonian) in the Alpine-Carpathian Foredeep and the Vienna Basin in Lower Austria – An example of a Coarse-grained Fluvial System. *Jahrbuch der Geologischen Bundesanstalt* 144, 191–221.

Nemčok M. & Lexa J. 1990: Evolution of the basin and range structure around the Žiar mountain range. *Geologica Carpathica* 41, 229–258.

Nemec W. & Steel R.J. 1988: What is a fan delta and have do we recognize it? In: W. Nemec, R.J. Steel (Eds.): Fan-Deltas: Sedimentology and Tectonic Settings. Blackie, Glasgow, 3–13.

Normandeau A., Lajeunesse P., Poiré A.G. & Francus P. 2016: Morphological expression of bedforms formed by supercritical sediment density flows on four fjord-lake deltas of the southeastern Canadian Shield (Eastern Canada). *Sedimentology* 63, 2106–2129. https://doi.org/10.1111/sed.12298

Patruno S. & Helland-Hansen W. 2018: Clinoforms and clinoform systems: Review and dynamic classification scheme for shorelines, subaqueous deltas, shelf edges and continental margins. *Earth-Science Reviews* 185, 202–233. https://doi.org/10.1016/j.earscirev.2018.05.016

Pierson T.C. & Costa J.E. 1987: A rheologic classification of subaerial sediment-water flows. In: . Costa J.E. & Wieczorek G.F. (Eds.): Debris flows/avalanches: process, recognition and mitigation. *Geological Society of America Reviews in Engineering Geology* 7, 1–12.

Postma G. 2009: Depositional Architecture and Facies of River and Fan Deltas: A Synthesis. In: Colella A. & Prior D.B. (Eds.): Coarse-Grained Deltas. *Blackwell Publishing Ltd.*, Oxford, 13–27.

Postma G. 2014: Generic autogenic behaviour in fluvial systems: Lessons from experimental studies. In: From Depositional Systems to Sedimentary Successions on the Norwegian Continental Margin, 1–18.

Postma G. & Cartigny M.J.B. 2014: Supercritical and subcritical turbidity currents and their deposits – A synthesis. *Geology* 42, 987–990. https://doi.org/10.1130/g35957.1

Postma G., Lang J., Hoyal D.C., Fedele J.J., Demko T., Abreu V. & Pederson K.H. 2021: Reconstruction of bedform dynamics controlled by supercritical flow in the channel–lobe transition zone of a deep-water delta (Sant Llorenç del Munt, north-east Spain, Eocene). *Sedimentology* 68, 1674–1697. https://doi.org/10.1111/sed.12735

Priechodská Z. & Harčár J. 1988: Explanation to Geological Map of the North-Eastern Part of the Podunajská Nížina Lowland, Scale 1:50,000. *Geologický Ústav Dionýza Štúra (Slovak State Geological Survey)*, Bratislava, 1–114 (in Slovak).

Raisbeck G.M., Yiou F., Fruneau M., Loiseaux J.M., Lievin M. & Ravel J.C. 1981: Cosmogenic ^{10}Be/^{7}Be as a probe of atmospheric transport processes. *Geophysical Research Letters* 8, 1015–1018.

Reesink A.J.H. 2018: Interpretation of cross strata formed by unit bars. In: Ghinassi M., Colombera L., Mountney N.P. & Reesink A.J.H. (Eds.): Fluvial Meanders and Their Sedimentary Products in the Rock Record. *International Association of Sedimentologists Special Publication, Wiley-Blackwell*, Oxford, 173–200.

Robert A. & Uhlman W. 2001: An experimental study on the ripple-dune transition. *Earth Surface Processes and Landforms* 26, 615–629. https://doi.org/10.1002/esp.211

Rosta É. 1993: Gilbert-type delta in the Sarmatian-Pannonian sediments, Sopron, NW-Hungary. *Földtani Közlöny* 123, 167–193.

Rybár S. & Kotulová J. 2023: Petroleum play types and source rocks in the Pannonian basin, insight from the Slovak part of the Danube Basin. *Marine and Petroleum Geology* 149, 106092. https://doi.org/10.1016/j.marpetgeo.2022.106092

Šarinová K., Rybár S., Halásová E., Hudáčková N., Jamrich M., Kováčová M. & Šujan M. 2018: Integrated biostratigraphical, sedimentological and provenance analyses with implications for lithostratigraphic ranking: The Miocene Komjatice depression of the Danube Basin. *Geologica Carpathica* 69, 382–409. https://doi.org/10.1515/geoca-2018-0023

Scholz C. A., Rosendahl B. R. & Scott D. L. 1990: Development of coarse-grained facies in lacustrine rift basins: Examples from East Africa. *Geology* 18, 140–144. https://doi.org/10.1130/0091-7613(1990)018<0140:DOCGFI>2.3.CO;2

Singleton A.A., Schmidt A.H., Bierman P.R., Rood D.H., Neilson T.B., Greene E.S., Bower J.A. & Perdrial N. 2017: Effects of grain size, mineralogy, and acid-extractable grain coatings on the distribution of the fallout radionuclides ^{7}Be, ^{10}Be, ^{137}Cs, and ^{210}Pb in river sediment. *Geochimica et Cosmochimica Acta* 197, 71–86. https://doi.org/10.1016/j.gca.2016.10.007

Slootman A. & Cartigny M.J.B. 2020: Cyclic steps: Review and aggradation-based classification. *Earth-Science Reviews* 201, 102949. https://doi.org/10.1016/j.earscirev.2019.102949

Slootman A., Vellinga A.J., Moscariello A. & Cartigny M.J.B. 2021: The depositional signature of high-aggradation chute-and-pool bedforms: The build-and-fill structure. *Sedimentology* 68, 1640–1673. https://doi.org/10.1111/sed.12843

Song Y., Ren J., Liu K., Lyu D., Feng X., Liu Y. & Stepashko A. 2022: Syn-rift to post-rift tectonic transition and drainage reorganization in continental rifting basins: Detrital zircon analysis from the Songliao Basin, NE China. *Geoscience Frontiers* 13, 101377. https://doi.org/10.1016/j.gsf.2022.101377

Spencer C.J., Yakymchuk C. & Ghaznavi M. 2017: Visualising data distributions with kernel density estimation and reduced chi-squared statistic. *Geoscience Frontiers* 8, 1247–1252. https://doi.org/10.1016/j.gsf.2017.05.002

Stoica M., Lazăr I., Krijgsman W., Vasiliev I., Jipa D. & Floroiu A. 2013: Paleoenvironmental evolution of the East Carpathian foredeep during the late Miocene-early Pliocene (Dacian Basin; Romania). *Global and Planetary Change* 103, 135–148. https://doi.org/10.1016/j.gloplacha.2012.04.004

Stow D.A. 2005: Sedimentary Rocks in the Field. A Colour Guide. *Manson Publishing*, London, 1–320.

Šujan M., Braucher R., Kováč M., Bourlès D.L., Rybár S., Guillou V. & Hudáčková N. 2016: Application of the authigenic $^{10}Be/^{9}Be$ dating method to Late Miocene–Pliocene sequences in the northern Danube Basin (Pannonian Basin System): Confirmation of heterochronous evolution of sedimentary environments. *Global and Planetary Change* 137, 35–53. https://doi.org/10.1016/j.gloplacha.2015.12.013

Šujan M., Braucher R., Tibenský M., Fordinál K., Rybár S. & Kováč M. 2020: Effects of spatially variable accommodation rate on channel belt distribution in an alluvial sequence: Authigenic $^{10}Be/^{9}Be$-based Bayesian age-depth models applied to the upper Miocene Volkovce Fm. (northern Pannonian Basin System, Slovakia). *Sedimentary Geology* 397, 105566. https://doi.org/10.1016/j.sedgeo.2019.105566

Šujan M., Braucher R., Mandic O., Fordinál K., Brixová B., Pipík R.K., Šimo V., Jamrich M., Rybár S., Klučiar T., Team A., Ruman A., Zvara I. & Kováč M. 2021a: Lake pannon transgression on the westernmost tip of the carpathians constrained by biostratigraphy and authigenic $^{10}Be/^{9}Be$ dating (central Europe). *Rivista Italiana di Paleontologia e Stratigrafia* 127, 627–653. https://doi.org/10.13130/2039-4942/16620

Šujan M., Rybár S., Kováč M., Bielik M., Majcin D., Minár J., Plašienka D., Nováková P. & Kotulová J. 2021b: The polyphase rifting and inversion of the Danube Basin revised. *Global and Planetary Change* 196, 103375. https://doi.org/10.1016/j.gloplacha.2020.103375

Šujan M., Aherwar K., Braucher R., Chyba A., Sztanó O., Vlček T., Hudáčková N., Jamrich M., Šarinová K. & AsterTeam 2023a: Redeposited mud in hybrid event beds hinder the applicability of the authigenic $^{10}Be/^{9}Be$ dating: eastern Danube Basin, Slovakia. 36th International Meeting of Sedimentology, Dubrovnik, Croatia, 387. https://doi.org/10.13140/RG.2.2.15447.04001

Šujan M., Braucher R., Chyba A., Vlačiky M., Aherwar K., Rózsová B., Fordinál K., Maglay J., Nagy A., Moravcová M. & AsterTeam 2023b: Mud redeposition during river incision as a factor affecting authigenic $^{10}Be/^{9}Be$ dating: Early Pleistocene large mammal fossil-bearing site Nová Vieska, eastern Danube Basin. *Journal of Quaternary Science* 38, 347–364. https://doi.org/10.1002/jqs.3482

Sztanó O., Magyar I., Szónoky M., Lantos M., Müller P., Lenkey L., Katona L. & Csillag G. 2013a: Tihany Formation in the surroundings of Lake Balaton: Type locality, depositional setting and stratigraphy. *Foldtani Kozlony* 143, 73–98.

Sztanó O., Szafian P., Magyar I., Horanyi A., Bada G., Hughes D.W., Hoyer D.L. & Wallis R.J. 2013b: Aggradation and progradation controlled clinothems and deep-water sand delivery model in the Neogene Lake Pannon, Mako Trough, Pannonian Basin, SE Hungary. *Global and Planetary Change* 103, 149–167. https://doi.org/10.1016/j.gloplacha.2012.05.026

Sztanó O., Kováč M., Magyar I., Šujan M., Fodor L., Uhrin A., Rybár S., Csillag G. & Tokés L. 2016: Late Miocene sedimentary record of the Danube/Kisalföld Basin: Interregional correlation of depositional systems, stratigraphy and structural evolution. *Geologica Carpathica* 67, 525–542. https://doi.org/10.1515/geoca-2016-0033

Tari G., Bada G., Boote D.R.D., Krézsek C., Koroknai B., Kovács G., Lemberkovics V., Sachsenhofer R.F. & Tóth T. 2023: The Pannonian Super Basin: A brief overview. *AAPG Bulletin* 107, 1391–1417. https://doi.org/10.1306/02172322098

ter Borgh M., Vasiliev I., Stoica M., Knežević S., Matenco L., Krijgsman W., Rundić L. & Cloetingh S. 2013: The isolation of the Pannonian basin (Central Paratethys): New constraints from magnetostratigraphy and biostratigraphy. *Global and Planetary Change* 103, 99–118. https://doi.org/10.1016/j.gloplacha.2012.10.001

Toonen W.H.J., Kleinhans M.G. & Cohen K.M. 2012: Sedimentary architecture of abandoned channel fills. *Earth Surface Processes and Landforms* 37, 459–472. https://doi.org/10.1002/esp.3189

Van Baak C.G.C., Mandic O., Lazar I., Stoica M. & Krijgsman W. 2015: The Slanicul de Buzau section, a unit stratotype for the Romanian stage of the Dacian Basin (Plio-Pleistocene, Eastern Paratethys). *Palaeogeography, Palaeoclimatology, Palaeoecology* 440, 594–613. https://doi.org/10.1016/j.palaeo.2015.09.022

Van Dijk M., Postma G. & Kleinhans M.G. 2009: Autocyclic behaviour of fan deltas: An analogue experimental study. *Sedimentology* 56, 1569–1589. https://doi.org/10.1111/j.1365-3091.2008.01047.x

Vasiliev I., de Leeuw A., Filipescu S., Krijgsman W., Kuiper K., Stoica M. & Briceag A. 2010: The age of the Sarmatian–Pannonian transition in the Transylvanian Basin (Central Paratethys). *Palaeogeography, Palaeoclimatology, Palaeoecology* 297, 54–69. https://doi.org/10.1016/j.palaeo.2010.07.015

Vaškovský I., Brestenská E. & Halouzka R. 1979: Vysvetlivky k listom geologických máp 1:25 000, listy Tekovské Lužany, Šárovce, Nýrovce, Želiezovce, čiastková záverečná správa. Úloha: Základný regionálny výskum kvartéru Západných Karpát. Manuscript, Geofond Nr. 45413, *State Geological Survey of Dionýz Štúr,* Bratislava, 1–67. Available online at: https://da.geology.sk/navigator/?desktop=Public

Vass D., Pereszlényi M., Kováč M. & Král M. 1990: Out-line of Danube Basin geology. *Földtani Közlöny* 120, 193–214.

Vendettuoli D., Clare M.A., Hughes Clarke J.E., Vellinga A., Hizzet J., Hage S., Cartigny M.J.B., Talling P.J., Waltham D., Hubbard S.M., Stacey C. & Lintern D.G. 2019: Daily bathymetric surveys document how stratigraphy is built and its extreme incompleteness in submarine channels. *Earth and Planetary Science Letters* 515, 231–247. https://doi.org/10.1016/j.epsl.2019.03.033

Voštiarová I. 2013: Vrchnomiocénne depozičné systémy komjatickej depresie Dunajskej panvy. *Diploma thesis. Faculty of Natural Sciences, Comenius University Bratislava,* 1–59. Available online at: https://opac.crzp.sk/?fn=detailBiblioFormChildU1G0HA&sid=ACAA4AF27E5710F225A8E222FFDC&seo=CRZP-detail-kniha

Wang N., Zhang Z., Malusà M.G., Zhang J., Wu L., Xiang D. & Xiao W. 2023: Geo-thermochronological analysis reveals transition from transverse to axial detrital inputs during Cretaceous rifting in the Songliao Basin, NE China. *Terra Nova*. https://doi.org/10.1111/ter.12682

Willenbring J.K. & von Blanckenburg F. 2010: Meteoric cosmogenic Beryllium-10 adsorbed to river sediment and soil: Applications for Earth-surface dynamics. *Earth-Science Reviews* 98, 105–122. https://doi.org/10.1016/j.earscirev.2009.10.008

Wittmann H., Von Blanckenburg F., Bouchez J., Dannhaus N., Naumann R., Christl M. & Gaillardet J. 2012: The dependence of meteoric ^{10}Be concentrations on particle size in Amazon River bed sediment and the extraction of reactive $^{10}Be/^{9}Be$ ratios. *Chemical Geology* 318–319, 126–138. https://doi.org/10.1016/j.chemgeo.2012.04.031

Wittmann H., von Blanckenburg F., Mohtadi M., Christl M. & Bernhardt A. 2017: The competition between coastal trace metal fluxes and oceanic mixing from the $^{10}Be/^{9}Be$ ratio: Implications for sedimentary records. *Geophysical Research Letters* 44, 8443–8452. https://doi.org/10.1002/2017GL074259

Yawar Z. & Schieber J. 2017: On the origin of silt laminae in laminated shales. *Sedimentary Geology* 360, 22–34. https://doi.org/10.1016/j.sedgeo.2017.09.001

Electronic supplementary material is available online as Mendeley dataset at https://doi.org/10.17632/svr45t2xtj.2